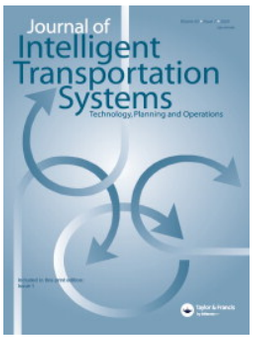

Taylor & Francis
Taylor & Francis Group

Journal of Intelligent Transportation Systems
Technology, Planning, and Operations

ISSN: 1547-2450 (Print) 1547-2442 (Online) Journal homepage: www.tandfonline.com/journals/gits20

Assessing the impacts of tradable credit schemes through agent-based simulation

Renming Liu, Dimitrios Argyros, Yu Jiang, Moshe E. Ben-Akiva, Ravi Seshadri & Carlos Lima Azevedo

To cite this article: Renming Liu, Dimitrios Argyros, Yu Jiang, Moshe E. Ben-Akiva, Ravi Seshadri & Carlos Lima Azevedo (26 May 2026): Assessing the impacts of tradable credit schemes through agent-based simulation, Journal of Intelligent Transportation Systems, DOI: 10.1080/15472450.2026.2669872

To link to this article: https://doi.org/10.1080/15472450.2026.2669872

Published online: 26 May 2026.

JOURNAL OF INTELLIGENT TRANSPORTATION SYSTEMS
https://doi.org/10.1080/15472450.2026.2669872

Assessing the impacts of tradable credit schemes through agent-based simulation

Renming Liu[a], Dimitrios Argyros[a], Yu Jiang[a], Moshe E. Ben-Akiva[b], Ravi Seshadri[a], and Carlos Lima Azevedo[a]

[a]Department of Technology, Management and Economics, Technical University of Denmark, Kongens Lyngby, Denmark; [b]Department of Civil and Environmental Engineering, Massachusetts Institute of Technology, Cambridge, MA, USA

ABSTRACT

Tradable credit schemes (TCS) are an alternative to congestion pricing, offering revenue neutrality and the potential to address equity concerns through the credit allocation. Past research on the performance of TCS has largely relied on simplified network and market equilibrium models that may fail to capture the complexities of transportation demand, supply, and credit market interactions. Agent- and activity-based simulation provides a more comprehensive approach by explicitly modeling individual traveler behaviors and market dynamics. This study proposes an integrated simulation framework for TCS implementation within the open-source urban simulation platform SimMobility, featuring: (a) a flexible TCS design that accounts for multiple trips and individual trading behaviors; (b) a simulation framework that models interactions between travelers, the TCS regulator, and the market; (c) TCS optimized using Gaussian Processes and Bayesian Optimization, and (d) simulation experiments on a large-scale mesoscopic multimodal network. Results show that network and market performance stabilize over time, aligning with theoretical TCS properties from network equilibrium models. We confirm the efficiency of TCS in reducing congestion and explore its varied impacts on users, travel behavior, and market dynamics. Our framework allows for designing different TCS configurations and testing their effect in mitigating potentially undesirable trading and market behavior, ultimately contributing to a closer-to-practice design and assessment.

ARTICLE HISTORY
Received 28 April 2025
Revised 12 December 2025
Accepted 2 May 2026

KEYWORDS
agent-based simulation; Bayesian optimization; demand management; Gaussian process; tradable credit scheme

1. Introduction

Travel demand management aims to reduce road traffic congestion by altering patterns of trip-making, activity participation, mode, departure time, and route choices, with congestion pricing being one of the most prominent measures. Although traditionally, congestion pricing has been popular in both theory and practice, with significant impact on route choices (Nielsen, 2004), traffic throughput (Lombardi et al., 2023), and demonstrable gains in social welfare (Lindsey, 2006), it often receives political and social resistance as it is perceived as a tax (de Palma & Lindsey, 2020). A tradable credit scheme (TCS) is a form of quantity control which offers an appealing alternative that has the potential of addressing the issues of political and social opposition if properly designed.

TCS provides a market-based mechanism that can be tightly integrated with Intelligent Transport Systems (ITS) to manage congestion and optimize network performance. Using ITS technologies, such as real-time traffic monitoring, vehicle-to-infrastructure communication, and dynamic routing, authorities can adjust credit requirements based on current traffic conditions, encouraging travelers to shift routes, times, or modes. This creates a responsive, data-driven system where congestion management is both efficient and flexible, aligning traveler behavior with overall network efficiency.

In a typical TCS system, a regulator provides an initial endowment of mobility credits to potential travelers. The credits can be bought and sold in a market monitored by the regulator at a price determined by demand and supply (Grant-Muller & Xu,

CONTACT Dimitrios Argyros diar@dtu.dk Department of Technology, Management and Economics, Technical University of Denmark, Kongens Lyngby, Denmark.

2014). Tradable credits provide two key advantages over congestion pricing without refunding: (1) there is no net financial flow from road users to the regulator, making it revenue-neutral and potentially less susceptible to political opposition; (2) in theory, it can achieve any desired equity distribution through the initial credit allocation, and it enables the regulator to directly control quantity (e.g., of road use) (Fan & Jiang, 2013). Since the early work of Goddard (1997); Verhoef et al. (1997), there has been a surge in academic attention toward TCS. For a comprehensive review of different TCS conceptualizations, designs, implementations, and credit distributions the reader is referred to Fan and Jiang (2013); Provoost et al. (2023); Servatius et al. (2023).

The review in Grant-Muller and Xu (2014) focuses on studies that formulate mathematical programming models to investigate user and market equilibrium considering transaction costs, fixed/elastic demand, and homogeneous/heterogeneous travelers. Dogterom et al. (2017) summarizes the empirical findings in individual behaviors under different TCS systems, including loss aversion, mental accounting and decision-making under uncertainty. Subsequent extensions include consideration of multi-period TCS (Miralinaghi & Peeta, 2016, 2018), cyclic TCS (Xiao et al., 2019), comparative analysis with congestion pricing (de Palma et al., 2018; Seshadri et al., 2022), dynamics of the credit price (Balzer & Leclercq, 2022; Guo et al., 2019; Liu et al., 2023; Ye & Yang, 2013), detailed individual market behaviors (namely, selling and buying) (Chen et al., 2023; Hamm et al., 2023; Tian et al., 2019), transaction costs in TCS (Fan et al., 2022; Zhang et al., 2021), multimodality in TCS (Balzer et al., 2023), and TCS for parking management (Alogdianakis et al., 2024; Bao & Ng, 2022; Liu et al., 2014; Xiao et al., 2021).

Despite the large body of research on TCS, there are several challenges that need to be addressed before real-world deployments are possible. First, most previous studies use simplistic demand and supply models for assessment and employ static equilibrium approaches to model the credit market (with the exception of Ye and Yang (2013); Guo et al. (2019); Balzer and Leclercq (2022); Liu et al. (2023) where the flow and credit price dynamics are captured). Thus, few attempts are made to model the disaggregate behavior of individuals within the market, let alone the modeling of behavioral responses such as loss aversion, budgeting, learning effects, etc. (Dogterom et al., 2017). Second, there is little research on the design of the credit system itself, namely, aspects such as credit allocation, trading, market regulation and transaction costs (Fan et al., 2022; Lessan & Fu, 2022; Nie, 2012), and the impacts on the system efficiency and individual behavior in the market.

To summarize, our current understanding of the impacts and operations of a TCS would benefit from a framework that captures the complex interactions among user behavior, regulator actions, and market design, and that provides comprehensive assessments of different TCS. In this paper, we contribute to the existing literature by: (a) proposing a flexible simulation-based framework to model a TCS including the explicit consideration of the disaggregate behavior of users and their interactions within the market and with the regulator (the framework also proposes a model of individual selling behavior that extends the one proposed in Chen et al. (2023) to consider multiple trips), (b) implementing the framework in a modular and extensible manner in the state-of-the-art urban simulator SimMobility (Adnan et al., 2016), allowing for the detailed simulation of the operations of a TCS system, and c) conducting simulation experiments using a prototypical city to showcase the functionality of the proposed framework and to yield insights into the impacts of TCS on congestion, scheme design, and market behavior.

SimMobility is an integrated agent- and activity-based simulation platform that uses a multi-scale framework comprising three primary modules at different temporal scales: Long-term (year-to-year) (Adnan et al., 2016), mid-term (day-to-day) (Lu et al., 2015a), and short-term (within day) (Azevedo et al., 2017). Specifically, SimMobility mid-term simulates agents' behavior, including their activity and travel patterns and the movement of vehicles and travelers. This study extends the mid-term module with new functionalities that can simulate the operations of a complex TCS system. Furthermore, it aligns closely with the capabilities of ITS. Real-time data flows and dynamic control mechanisms would enable a TCS to function effectively in practice. By modeling individual traveler behaviors and system-wide interactions, the agent-based simulation mirrors how a TCS would operate within an ITS environment, allowing us to evaluate responsiveness and network performance under realistic conditions.

The rest of this paper is structured as follows. In Section 2, we introduce the TCS design and the proposed market behavior model, which includes deriving an optimal selling strategy considering multiple daily trips. The architecture of the SimMobility mid-term module and its core design components are discussed

in Section 3. Section 4 describes the optimization formulation to determine the credit charging scheme (toll profile in credits). Next, simulation results are discussed in Section 5, followed by conclusions and directions for future research in Section 6.

2. TCS framework

The TCS we consider in our simulation framework extends the design presented in Brands et al. (2020) and Chen et al. (2023) to incorporate multiple trips within a day. The framework is generic and allows for various toll designs including distance-based, area-based and cordon-based schemes. For the sake of completeness, we outline the interactions of stakeholders in an operational system for TCS in Section 2.1, then provide a summary of the TCS/market design in Section 2.2 and describe our proposed extensions for agent-based and network simulation in Section 2.3.

2.1. Interactions of travelers, the market and the regulator

An operational system for TCS contains three types of actors or agents: travelers, the regulator, and a market platform. The regulator distributes credits to all travelers at a certain rate r. At a given time t, travelers determine their roles as either sellers or buyers depending on the account balance and the credit needs associated with their mobility choices. Note that the buying and selling decisions of users may be suitably automated through a smartphone application since in practice it is unrealistic to expect users to constantly interact with the system. The models described in Section 2.3 should be interpreted in this sense, namely that they represent strategies that could be automated through a smartphone.

We design a market platform agent, which handles, collects and records all transactions, and interacts with both travelers and the regulator. Travelers need to send trading requests through the market platform to the regulator and proceed with the transactions after approval. This entails several checks, for instance, a buying request might be rejected if the cap of credit usage has been reached, and a selling request could be rejected if the regulator's revenue is lower than a predetermined threshold. These processes also underlie the adjustment of credit price, which again is not the responsibility of the regulator, but a result of credit demand-supply interactions, using the collected transaction information on a daily basis.

The overall framework of interactions is shown in Figure 1. In Section 3.2, we will introduce in detail the design of classes, functions, and the information synchronization established based on the interaction framework in the simulation platform.

2.2. TCS design

The TCS system we consider has the following features:

Credit allocation: We use a 'continuous' allocation approach wherein the regulator gives out credits to every traveler at a certain rate over the entire day. Compared to a lump-sum allocation (Brands et al., 2020), the 'continuous' allocation can potentially prevent concentrated trading activities due to credit expiration and provides additional degrees of freedom to the regulator to intervene in the market (Chen et al., 2023). The lump-sum allocation often used in the literature (Brands et al., 2020) is a special case of the 'continuous' allocation where the allocation interval is relatively large (for example, one day).

Credit expiration: Each credit has a certain initial lifetime specified by the regulator. The expiration of credits can avoid speculative behavior in the market,

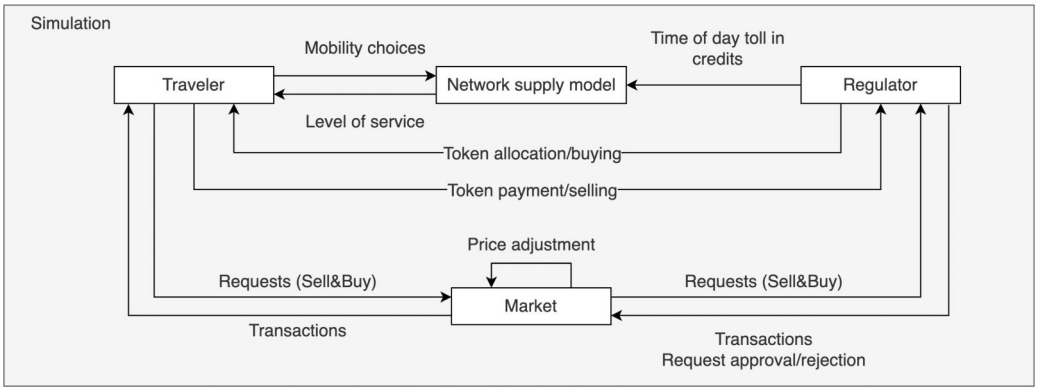

Figure 1. Interactions between the travelers, regulator, and market.

such as credit stocking and banking (de Palma & Lindsey, 2020).

Credit transactions: All travelers are assumed to trade directly with the regulator, who guarantees all buying and selling requests. Such a 'traveler-to-regulator' trading mechanism is beneficial in reducing transaction costs associated with information acquisition, negotiation, and other peer-to-peer trading and auctioning features (Brands et al., 2020). Thus, travelers who are short of credits can only buy the remaining credits needed at departure and for immediate use. Furthermore, when a traveler wishes to sell credits to the regulator, he or she has to sell all credits in the credit account. Finally, travelers are not allowed to sell and buy credits at the same time. For a more detailed discussion of the implications of these assumptions, we refer the reader to Chen et al. (2023).

Credit toll: When the toll is active, travelers have to pay the toll in credits to use the road network. The toll in credits charged by the regulator is dynamic and varies by time of day but is invariant across days. It can further be either distance-based, area-based, cordon-based or a combination of these. An upfront credit toll at departure is used for all trips.

Each traveler possesses a credit account, whose balance evolves over time. Let r denote the allocation rate of credits, l be the credit lifetime, and $x_n^d(t)$ be traveler n's credit account balance at time t on day d. The maximum number of credits accumulated in the account is $l \cdot r$. Once an account has reached this state (referred to as '*full wallet*' hereafter), the balance does not change in the absence of selling or traveling, as every time a new credit is acquired, the oldest credit expires. In contrast, when the account balance is smaller than $l \cdot r$, it increases by $r \cdot \Delta t$ in a time interval Δt. Let $g(t)$ denote the credit toll at time t and $t_{n,i,d}^{dep}$ be the departure time of traveler n's ith trip on the day d. Note that at time t on the day d, traveler n can perform one and only one of the three actions that affect the account balance: start a trip (and possibly buy credits), do nothing, or sell all credits. We can then derive the account balance at time $t + \Delta t$ as follows:

A. Start a trip when $t = t_{n,i,d}^{dep}$
   - if $x_n^d(t) \geq g(t)$, traveler n's account balance at time $t + \Delta t$ is given by:

$$x_n^d(t + \Delta t) = \min(x_n^d(t) - g(t) + r \cdot \Delta t, l \cdot r). \quad (1)$$

   - if $x_n^d(t) \leq g(t)$, traveler n needs to buy $g(t) - x_n^d(t)$ credits, and the account balance at time $t + \Delta t$ is:

$$x_n^d(t + \Delta t) = r \cdot \Delta t, \quad (2)$$

as all credits in the account and bought credits are consumed for the trip.

B. Do nothing. The account balance $x_n^d(t + \Delta t)$ becomes:

$$x_n^d(t + \Delta t) = \min(x_n^d(t) + r \cdot \Delta t, l \cdot r). \quad (3)$$

C. Sell all credits $x_n^d(t)$, then:

$$x_n^d(t + \Delta t) = r \cdot \Delta t. \quad (4)$$

Credit price: As credits are bought and sold in a market, the price is determined endogenously by credit demand-supply interactions (Yang & Wang, 2011). We use the price adjustment mechanism from Liu et al. (2023) where the credit price is adjusted from day to day but fixed within a day. Specifically, the price on day d, p_d, increases or decreases proportionally to the previous day's excess credit consumption Z_d, defined as the difference between the total numbers of bought and sold credits by all travelers. Thus,

$$p_{d+1} = \max\{p_d + k * Z_d, 0\}, \quad (5)$$

where k is the price adjustment parameter. When the credit demand exceeds supply, the market price increases, and vice versa.

2.3. User's market behavior

We assume that the regulator levies a transaction fee on each transaction (buying and selling), which is composed of two parts, a fixed fee and a fee proportional to the value of traded credits. Let $f_b, f_s \geq 0$ and $\hat{f}_b, \hat{f}_s \geq 0$ denote the fixed and proportional fees for selling and buying transactions, respectively. We can write the revenue S of selling y credits with transaction fees on day d as:

$$S(y|p_d, f_s, \hat{f}_s) = y \cdot p_d \cdot (1 - \hat{f}_s) - f_s. \quad (6)$$

Similarly, the cost B of buying y credits with transaction fees on day d is given by:

$$B(y|p_d, f_s, \hat{f}_s) = y \cdot p_d \cdot (1 + \hat{f}_b) + f_b. \quad (7)$$

As described in Section 2.2, a buying transaction may only happen when a traveler starts its trip, while a selling transaction can occur at every time interval. Here we adopt the heuristic selling model from Chen et al. (2023), where an individual's selling strategy is developed by considering only one trip per day (i.e., the morning commute trip). We extend this

model to accommodate multiple trips and activities in a single day. At time t on day d, assume traveler n has I upcoming trips at times denoted by $t^{dep}_{n,i,d}, i = 1,2,...,I$; the expected profit of selling all credits at time $t < t^{dep}_{n,1,d}$ on day d without further selling, $P^d_n(t)$, can be written as follows,

$$\begin{aligned} P^d_n(t) &= S(x^d_n(t)) - \sum_{i=1}^{I} 1(g(t^{dep}_{n,i,d}) > x^d_n(t^{dep}_{n,i,d})) \cdot B(g(t^{dep}_{n,i,d}) - x^d_n(t^{dep}_{n,i,d})) \\ &= x^d_n(t) \cdot p_d \cdot (1 - \hat{f}_s) - f_s \\ &\quad - \sum_{i=1}^{I} 1(g(t^{dep}_{n,i,d}) > x^d_n(t^{dep}_{n,i,d})) \cdot ((g(t^{dep}_{n,i,d}) - x^d_n(t^{dep}_{n,i,d})) \cdot p_d \cdot (1 + \hat{f}_b) + f_b), \end{aligned} \tag{8}$$

where the expected account balance at the departure time of trip i is given by (recall that traveler n is assumed to have sold all of her credits at time t),
where $t < t^{dep}_{n,1,d}$. Note that the buying cost is only

Algorithm 1: Selling Strategy

Inputs : $d, t, n, p_d, t^{dep}_{n,i,d}, x^d_n(t), l, r, f_b, f_s, \hat{f}_b, \hat{f}_s$
At time t on day d, calculate $P^d_n(t)$ (Equation 8) ;
  and expected account balance at $t^{dep}_{n,i,d}$, $x^d_n(t^{dep}_{n,i,d})$ (Equation 9);
if $P^d_n(t) > 0$ **then**
  if $\exists i = 1,2,...,I$ such that $g(t^{dep}_{n,i,d}) \geq x^d_n(t^{dep}_{n,i,d})$ **then**
    Sell now;
  if $g(t^{dep}_{n,i,d}) < x^d_n(t^{dep}_{n,i,d}) \forall i = 1,2,...,I$ **then**
    Do nothing;
  if $x^d_n(t) = l \cdot r$ **then**
    Sell now;
else
  Do nothing;
end if

$$x^d_n(t^{dep}_{n,i,d}) = \begin{cases} \min\{(t^{dep}_{n,1,d} - t) \cdot r, l \cdot r\}, & i = 1, \\ \min\{\max\{x^d_n(t^{dep}_{n,i-1,d}) - g(t^{dep}_{n,i-1,d}), 0\} + (t^{dep}_{n,i,d} - t^{dep}_{n,i-1,d})r, l \cdot r\}, & i = 2,...,I, \end{cases} \tag{9}$$

incurred when the toll for trip i on day d, $g(t^{dep}_{n,i,d})$, is larger than the account balance at the time of departure of trip i, $x^d_n(t^{dep}_{n,i,d})$, as written by the indicator function in Equation (8). A critical assumption made for computing the selling profit is that there is no further selling until the last trip of the trip chain, which consists of I trips on day d and duplicated I trips on day $d+1$. Given the '*sell all credits*' rule and the presence of transaction fees, it is a justifiable assumption that allows us to derive the optimal selling strategy analytically.

In the presence of transaction costs, an optimal selling strategy for traveler n at time t on the day d can be derived (see Appendix A for a proof) and is summarized in Algorithm 1. The selling strategy involves checking several conditions at time t, which is discretized into one-minute intervals in the supply simulation. Thus, at the beginning of each one-minute interval, depending on which combination of conditions in Algorithm 1 is met either a decision to sell or a decision to not sell will be made. Note that this selling strategy is essentially myopic since no further selling is considered. This can be considered using a more complex dynamic programming formulation, however, we defer that into future research.

3. Simulation platform and design

SimMobility is an agent- and activity-based multi-level urban transportation simulation platform with an open-source codebase. SimMobility consists of three simulators at different temporal dimensions: The Long-term module simulates the evolution of population synthesis, residential and workplace locations, vehicle ownership, density, and land use distribution over a long period (typically from months to years) (Zhu et al., 2018); the Mid-term module covers daily activity scheduling, mode, route, destination and departure time choices on a multi-modal network (Lu et al., 2015a); finally, the Short-term module captures the vehicle behaviors on the road network at a high spatial-temporal resolution (in the order of milliseconds), including lane-changing, braking and accelerating, and device-to-device communications, and synthesizes traffic control and management systems (Azevedo et al., 2017). These three simulators are integrated in a way that decisions made in longer terms (e.g., Long-term) are inputs to decision-making in shorter terms (e.g., Mid-term), which, in turn, affect longer terms by providing supporting information (e.g., accessibility measures) (Adnan et al., 2016). SimMobility has been successfully applied to study

large networks and to design different congestion pricing strategies (Jing et al., 2024), thus the design and development of flexible TCS simulation capabilities within SimMobility provides a wide range of assessment opportunities from a demand-side perspective compared to other existing frameworks (Anda et al., 2017).

3.1. Overview of SimMobility mid-term

In this paper, we focus our development on the extension of SimMobility Mid-term for a wide range of TCS simulations. SimMobility Mid-term[1] is an open-source mesoscopic simulator that models agents' daily activities at the individual level on the demand side and simulates the movement at the mesoscopic level on the supply side (Adnan et al., 2016). SimMobility Mid-term comprises three main modules: *Pre-day*, *Within-day*, and *Supply*, shown as Figure 2.

The *Pre-day* module adopts the Day Activity Schedule approach (Bowman & Ben-Akiva, 2001) to predict the individual daily activity schedule, including activity type and number, activity duration and time of day (by half-hour time intervals), activity locations, and modes (Siyu, 2015). Given the information from the *Pre-day* output, the *Within-day* module extracts the trip chains and simulates travelers' departure time and route choice decisions before their trips as well as en-route decisions. The *Supply* module, which is a mesoscopic multi-modal traffic simulator, takes in the trip chains and simulates the actual movement trajectories. In the experiments in Section 5, we assume that the *Pre-day* activity schedules are fixed and focus on the *Within-day* module, which is described in Section 3.3.

3.2. Main components design

SimMobility is highly modularized and extensible so that we can expand the existing class definitions of agents and entities (Adnan et al., 2016) to add functionality *via* new classes, class attributes, operations, and associations between classes.

The base class used in SimMobility is termed '*Entity*', which encapsulates fundamental attributes such as its id, and functions such as the *update* function, which is called at every time step of the simulation. An entity may also be a message handler that can receive and react to messages coordinated by a messaging system. Derived from '*Entity*', class '*Agent*' forms the base for all SimMobility Mid-term agents, including persons, traffic lights, loop-detectors, bus-stop agents, etc. The reader is referred to both Adnan et al. (2016) and footnote 1 for further details on SimMobility architecture. To establish the operational system for TCS, five main components need to be

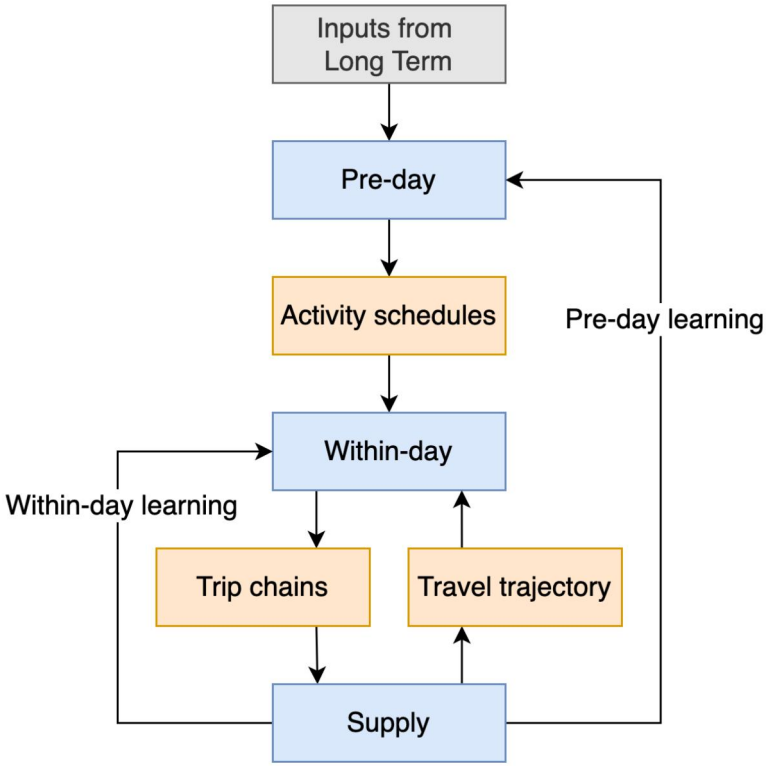

Figure 2. SimMobility mid-term framework.

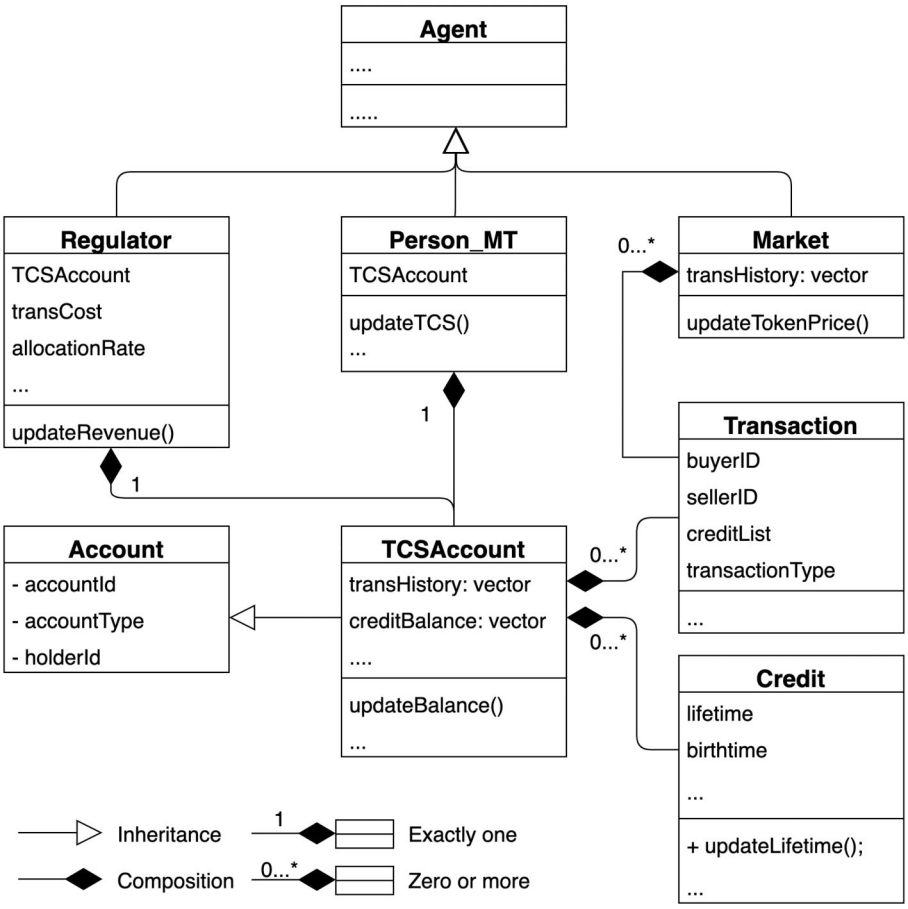

Figure 3. Class diagram of the TCS framework in SimMobility.

added to the SimMobility Mid-term simulator: individual TCS accounts, a regulator, a market, the credits and all its related transactions.

Figure 3 illustrates the proposed TCS system structure by a class diagram containing each class's main attributes and operations. We define a generic '*Account*' class with basic attributes, including the account ID, account type, and owner ID. Different account types can be used for the purposes of simulating different policies (e.g., user account used for subscriptions and product choices in a congestion pricing or Mobility-as-a-Service setting (Kamargianni et al., 2019)). In the case of TCS, the account inherits from the base account class and contains the active credits and transaction records as vectors, as well as auxiliary variables such as numbers of used/bought/sold credits, transaction type, and numbers, and current predicted selling profit. A transaction object is generated when credits are traded or allocated, recording the transaction type (buy, sell, use, and allocation), buyer and seller IDs, and the list of credits. Credits are generated by the regulator and have a birth time and lifetime, which is updated as the simulation proceeds. The new regulator and market, as well as the existing traveler (Person MT) inherit from the base agent class in SimMobility. The regulator has its own TCS account, specifies the allocation rate and transaction costs, and records the revenue from trading with travelers. Each traveler also has her own account and updates it every time a transaction or expiration of credits occurs. The market collects information on all transactions between travelers and the regulator and adjusts the credit price accordingly.

Following the interactions described in Section 2.1, the design of communications among the regulator, market and travelers is shown in the sequence diagram Figure 4. At each time step, the regulator and traveler check for the occurrence of the four possible types of transactions in sequence, specifically, credit allocation first, followed by buying (if needed) and using transactions, and finally selling of credits. The 'continuous' allocation is discretized for a specified time interval, as small as the simulation time step itself (to be optimized for computational efficiency). An allocation is triggered when the current time equals the start time of such predetermined allocation time interval. The regulator sends the credits to all travelers and broadcasts the information to the

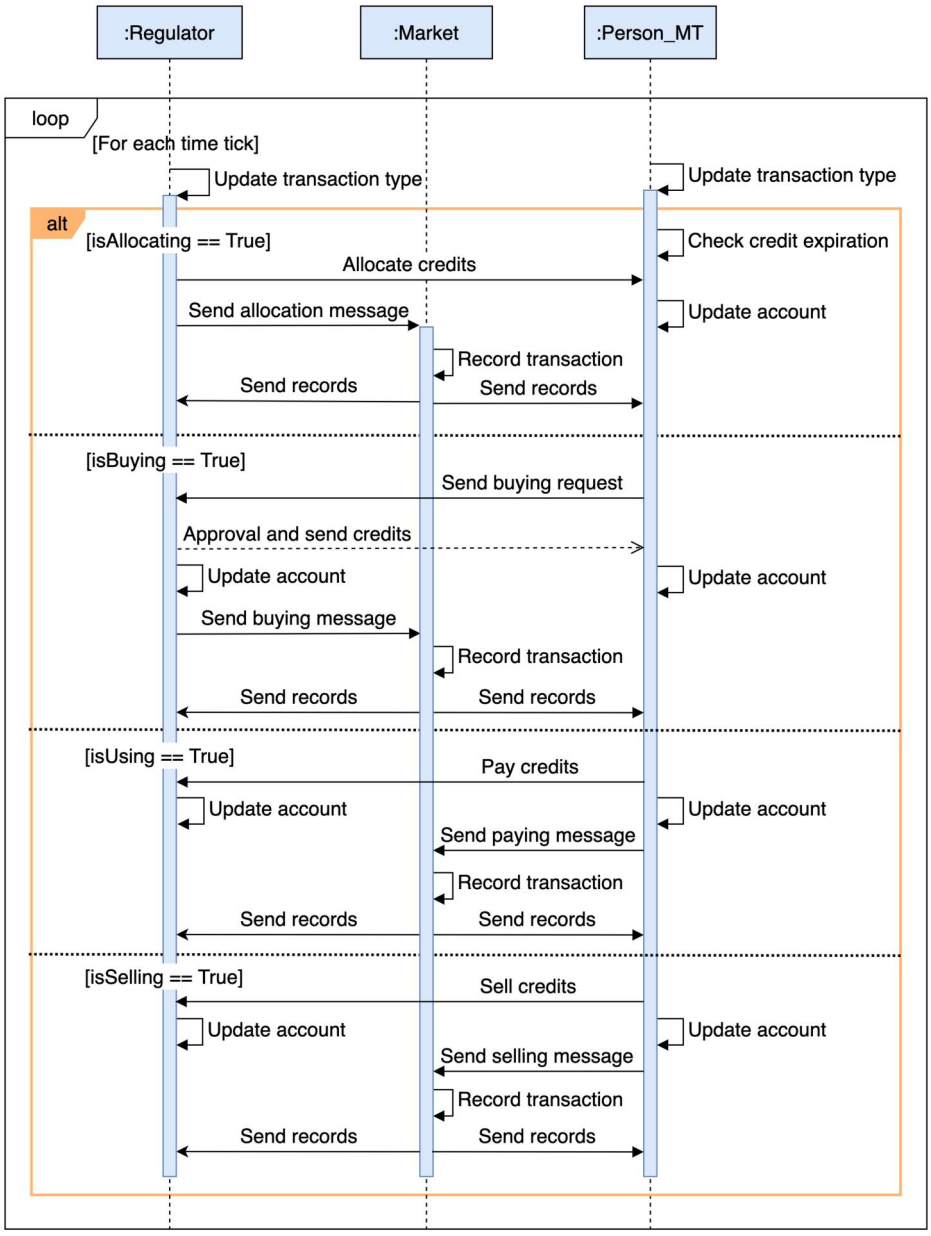

Figure 4. Sequence diagram for information exchanges under the TCS framework in SimMobility.

market, which generates a transaction record and sends it to both the regulator and travelers. Travelers will update their account balances after receiving the credits. Note that in the same time tick, the credit expiration check is automatically conducted (credits can only expire within the allocation interval when the credit lifetime is an integer multiple of that interval, a general design that also avoids unnecessary computations). For the buying and using case, the use of credits is triggered by the departure time of a trip, and the buying of credits is triggered only when the traveler is short of credits. For a buying transaction, a traveler sends the buying request stating the number of credits, and the regulator sends back the credits upon approval of the request, sending the trading information to the market at the same time. Both the regulator and traveler update their account and receive the transaction record from the market after the trade. Similarly, in the case of using and selling credits, travelers transfer credits to the regulator, and the market records the transaction information. After a certain period, the market will use the aggregated information to adjust the credit price based on the rule specified in Section 2.2. In this paper, we set the period as a day and defer the within-day price adjustment to future tests.

All the communication of information happens through the SimMobility messaging system (Adnan

et al., 2016), which collects the messages from all senders and distributes them to related receivers. The above architecture is generic enough and can be easily extended to handle any possible TCS designs, particularly peer-to-peer (P2P) trading mechanisms. A P2P trading mechanism with auction-based credit pricing could possibly be implemented as follows (Liu et al., 2024): all travelers send their buying or selling requests containing the number of needed (or surplus) credits and the bidding (or offer) price to the market, which acts as a coordination platform (with additional functions) that sorts all requests, matches the buyers and sellers with transaction price determined by the matched orders (for example, the average value of the bid and offer prices (Wörner et al., 2022)), and subsequently sends the matching messages to related travelers. Upon receiving the matching message, sellers send credits to buyers and transaction records to the market. When the total credit supply is smaller than the demand, the regulator may be involved in transactions which it sells credits to buyers at a ceiling price that is higher than the highest offer price. The corresponding messaging process is similar to the one we describe in Figure 4.

3.3. Demand model extensions

The proposed demand model (pre-trip decision) is a combined departure time and route choice model. Assume that each traveler n has a preferred arrival time $T^*_{n,i,d}$ for trip i on day d. We assume the preferred arrival time is unchanged across days. The departure time choice set is individual-specific and defined as:

$$TW_{n,i,d} = \{\hat{t}_{n,i,d} - \eta\Delta_{tw}, \hat{t}_{n,i,d} - (\eta-1)\Delta_{tw}, ..., \hat{t}_{n,i,d} + \eta\Delta_{tw}\}, \tag{10}$$

where η is the size parameter, and $\hat{t}_{n,i,d}$ is traveler n's preferred departure time interval on day d for trip i. Thus, the departure time window (choice set) $TW_{n,i,d}$ consists of $2\eta+1$ time intervals of size Δ_{tw} centered around the preferred departure time, $\hat{t}_{n,i,d}$, which is the preferred arrival minus an estimated travel time. The size parameters of the time window ($\eta \in \mathbb{Z}$) and time interval (Δ_{tw}) are configurable. It is noteworthy that all activities and intermediate trips in the given trip chain from the *Pre-day* module are performed in sequence, and hence a trip might be delayed by its previous trips. In other words, the end time of the previous activity, which is conducted after trip $i-1$ and before trip i, could be later than the edge of the time window of the current trip i, $\hat{t}_{n,i,d} - \eta\Delta_{tw}$. In this case, to maintain the number of departure time alternatives, we need to either shift the time window to the activity end time or shorten the activity duration or do both. This requires a more detailed model to account for the activity type (mandatory and discretionary) and the penalty of shifting the time window and shortening the activity. We defer this time window positioning problem to future research. In this study, we keep the activity duration unchanged and always shift the time window when needed.

The set of alternative paths between a given origin-destination node pair is generated *via* a combined method that uses the link elimination method, labeling method, k-shortest path method, and simulation method (Lu et al., 2015a). The choice set $\mathcal{K}$ of the combined departure time and route choice model is a product of the time window and path set. The combined departure time and route choice model uses the multinomial logit model.

The utility $U_{k,n,i,d}$ and its systematic part $V_{k,n,i,d}$ of choosing alternative k to traveler n for a given trip i on day d are, respectively:

$$U_{k,n,i,d} = V_{k,n,i,d} + \epsilon_{k,n,i,d}, \tag{11}$$

$$\begin{aligned} V_{k,n,i,d} = {} & \beta_{TT} \cdot TT_{k,n,i,d} \\ & + \delta_{n,i,d}\beta_{SDE,n} \cdot (T^*_{n,i,d} - t_k - TT_{k,n,i,d}) \\ & + (1-\delta_{n,i,d})\beta_{SDL,n} \cdot (t_k + TT_{k,n,i,d} - T^*_{n,i,d}) \\ & + \beta_{cost,n} \cdot g(t_k) \cdot p_d \cdot Dist_k \\ & + \beta_{PS} \cdot P\_size_k \\ & + \beta_{L} \cdot Dist_k \\ & + \beta_{sigNum} \cdot Sig\_num_k \\ & + \beta_{hwy\_dist} \cdot Hwy\_dist_k \\ & + \beta_{minTT,k} \cdot \text{Min}\_TT_k \\ & + \beta_{minDist} \cdot \text{Min}\_dist_k \\ & + \beta_{minSig} \cdot \text{Min}\_sig_k \\ & + \beta_{maxHwy} \cdot \text{Max}\_hwy_k, \\ & k \in \mathcal{K}, \end{aligned} \tag{12}$$

In summary, the systematic utility depends on travel time, schedule delay—both for early and late arrivals relative to a preferred arrival time—the cost associated with a departure time–dependent, distance-based TCS charge, and a path size attribute that captures correlations among overlapping routes. Additionally, it incorporates several route characteristics represented as binary indicators, including shortest travel time, shortest distance, fewest signals, and highest highway usage (Ben-Akiva & Bierlaire, 2003). The variables are described in detail below.

$TT_{k,n,i,d}$: Travel time of choosing alternative k, which specifies the departure time t_k and the route.

$\delta_{n,i,d}$: Binary variable, $\delta_{n,i,d} = 1$ when the arrival time is smaller the preferred arrival time, i.e., $t_k + TT_{k,n,i,d} < T^*_{n,i,d}$, otherwise $\delta_{n,i,d} = 0$.

$g(t_k) \cdot p_d \cdot Dist_k$: monetary value of the distance-based credit charge departing at t_k.

P_size_k: Path size the route from alternative k.

Sig_num_k: Number of signals in the route from alternative k.

Hwy_dist_k: Distance of the highway portion in the route from alternative k.

Min_TT_k: Binary variable, $\text{Min}\_TT_k = 1$ when this route have the shortest travel time in the set, otherwise $\text{Min}\_TT_k = 0$.

Min_dist_k: Binary variable, $\text{Min}\_dist_k = 1$ when this route have the shortest distance in the set, otherwise $\text{Min}\_dist_k = 0$.

Min_sig_k: Binary variable, $\text{Min}\_sig_k = 1$ when this route have the minimum number of signals in the set, otherwise $\text{Min}\_sig_k = 0$.

Max_hwy_k: Binary variable, $\text{Max}\_hwy_k = 1$ when route have the largest highway usage in the set, otherwise $\text{Max}\_hwy_k = 0$.

$\beta_{cost,n}$: Coefficient of toll cost, computed by $\frac{\beta_{TT}}{VOT_n}$, where the units are $\beta_{cost,n}$ (utility unit per minute) β_{TT} (minute), and value of time (VOT, unit: \$/minute).

$\beta_{sde,n}, \beta_{sdl,n}$: Coefficients of schedule delay early and late utility, computed by $\beta_{cost,n} \cdot SDE_n$ and $\beta_{cost,n} \cdot SDL_n$, respectively, where SDE_n and SDL_n (unit: \$/minute) are the monetary schedule delay early and late parameters.

$\epsilon_{k,n,i,d}$: Identically and independently Gumbel distributed random component.

$\beta_{TT}, \beta_L, \beta_{PS}, \beta_{sigNum}, \beta_{hwy\_dist}, \beta_{minTT,k}, \beta_{minDist}, \beta_{minSig}, \beta_{maxHwy}$: Calibrated model parameters.

In this study, we do not consider nonlinear income effects as in Chen et al. (2023); the allocation of credits is then a constant, not affecting the choice and thus, is not included in the utility function.

In the mid-term *With-day* module, a combined departure time and route choice is only made when the time approaches the time window of the corresponding trip. When applying the trading model in Section 2.3, the departure time of a future trip i, $t^{dep}_{n,i,d}$, is assumed to be the generated preferred departure time $\hat{t}_{n,i,d}$ unless the departure time is chosen. Thus the credit charge $g(t^{dep}_{n,i,d})$ and account balance $x^d_n(t^{dep}_{n,i,d})$ in Equation (8) are predicted values unless the time approaches the time window of the next trip, i.e., $t = \hat{t}_{n,i,d} - \eta\Delta_{tw}$. In addition, the selling model takes the trips on day d and $d+1$ into consideration, wherein the latter are assumed to be duplicates of the former.

3.4. Supply and day-to-day learning

The supply simulator in SimMobility mid-term follows the design of DynaMIT supply model (Ben-Akiva et al., 2002; Lu et al., 2015b), which includes private cars and buses. The mesoscopic road traffic network in SimMobility mid-term is represented by a hierarchical structure composed of links, segments, lane groups, and lanes. Each link is composed of several segments which represent a section of homogeneous roadway, which is further divided into two traffic flow regions: a moving part and a queuing part. Vehicles in the moving part travel at some uniform positive speed determined by a predefined macroscopic speed-density function, while vehicles in the queuing part form a spatial queue whenever the arrival rate exceeds the segment capacity. The reader is referred to Lu et al. (2015a) for further details on the mesoscopic supply simulator of SimMobility Mid-term.

SimMobility mid-term has a two-level learning framework as shown in Figure 2. In the upper level (pre-day learning), the aggregate zone-to-zone traffic performance indicators, including travel cost, travel time, travel distance, and waiting time for different modes (e.g., car, public transit, on-demand services, etc.) feedback to the *Pre-day* model to update agent's knowledge. In the lower level learning (within-day learning), the time-dependent link travel time can be iteratively updated considering a fixed *Pre-day* demand and used in the *Within-day* and *Supply* in-simulation interaction when agents have to make the combined departure time and (link-level) route choices. Both pre-day and within-day loops stop until consistency is achieved (Basu et al., 2021). In this study, we focus on the within-day day-to-day learning and keep the pre-day output (i.e., demand) fixed. An exponential smoothing filter is adopted to update the time-dependent link travel time, and the learning rate is the weight coefficient of the simulated (or realized) travel time. A larger learning rate leads to a more unstable system (Cantarella & Cascetta, 1995).

4. Bayesian optimization of TCS

Bayesian optimization (BO) is an efficient method for optimizing tolls in computationally intensive simulators like SimMobility, as introduced by Liu et al. (2020) and implemented in SimMobility by Argyros et al. (2023) for congestion pricing. BO's main element is a model of the objective function and an acquisition function.

4.1. Bayesian optimization formulation

A Gaussian process (GP) regression is used to model the objective function as in Equation (14). GP regression is defined by a prior mean function $\mu(x)$ and a covariance function $\kappa(x, x')$, with x, x' representing input variables related to the toll profile. Then, given a set of evaluated points, the GP is able to approximate the objective function, which in our case will be the social welfare (SW). The SW on a given day d is calculated based on the observed individual travel utilities (Equation (11)) with reference to the no-toll baseline considering the initial free token allocation. The result is then divided by the cost coefficient to convert it into monetary units. Thus, we have,

$$SW_d = \sum_{n,i} \frac{(U_{k^*_{i,n},n,i,d} - \beta_{cost,n} \cdot g(t_{k^*_{i,n}}) \cdot p_d \cdot Dist_{k^*_{i,n}}) - U^{*,base}_{n,i,d}}{|\beta_{cost,n}|}, \tag{13}$$

where $k^*_{i,n}$ represents the chosen alternative for individual n and trip i under the toll scenario and $U^{*,base}_{n,i,d}$ represents the corresponding utility of the chosen alternative in the base (no toll) scenario. To account for stochasticity of the simulator, we average the quantity in Equation (13) over multiple days after convergence to obtain the social welfare (denoted SW).

Thus, within BO, a GP is trained to approximate the SW:

$$SW_{(x)} \sim GP(\mu(x), \kappa(x, x')) \tag{14}$$

Moreover, the Matérn kernel (15) is used for the covariance function, as it has been adopted in prior TCS optimization work (Liu et al., 2023), suggesting its suitability for similar applications even though alternative kernels were not explicitly compared.

$$k(x, x') = \frac{2^{\nu-1}}{\Gamma(\nu)} \left(\frac{\sqrt{2\nu}}{l} |x - x'| \right)^{\nu} H_\nu \left(\frac{\sqrt{2\nu}}{l} |x - x'| \right) \tag{15}$$

where $\Gamma(\cdot)$ is the Gamma function and H_ν is the modified Bessel function, with $\nu = 5/2$ used.

The acquisition function determines the next point to evaluate (x_{next}) based on the posterior mean function and the variance of the Gaussian Process (GP). A commonly used acquisition function is the Upper Confidence Bound (UCB) presented in Equation (16) (Srinivas et al., 2012).

$$n_{(UCB)}(x, \rho) = -\mu(x) + \rho\sigma(x) \tag{16}$$

The hyperparameter ρ controls the balance between exploration and exploitation, with larger values of ρ indicating greater exploration. In this context, ρ equal to 2 was selected following Liu et al. (2020). Thus, the next point to evaluate is determined by maximizing the acquisition function as:

$$x_{next} = *argmax_x n_{(UCB)}(x, \rho) \tag{17}$$

4.2. BO extension for SimMobility

The integration framework of Bayesian Optimization (BO) with SimMobility for tolling optimization is illustrated in Figure 5 (Argyros et al., 2023). Here, we focus on within-day analysis, thus excluding the pre-day phase. In this framework, the knowledge about link travel times is updated and the social welfare is calculated for each within-day iteration. When consistency (equilibrium) is achieved, BO uses the average social welfare value from several within-day (i.e., to account for stochasticity in the simulator) iterations as input for the GP and produces a new toll. A Gaussian curve is employed to generate the new distance-based, time-varying credit toll $g(t)$ (unit: credits/meter) in the form of a (non-negative) step toll whose rate varies every 5 min. Specifically, three variables are considered for the BO processes: the amplitude (A_g), which represents the highest toll price; the mean (μ_g), which indicates the time at which this peak price occurs; and the standard deviation (σ_g) which defines the spread of the toll prices around the mean. Next, the framework initializes the link travel time knowledge in the database to the no-toll case and applies the new toll rates to the network. Lastly, set D represents an initial sample of tolls and their respective welfare values that are used to increase BO's efficiency and are updated for each new tested toll.

5. Experiment results

5.1. Study area and experimental design

This case study is tested using the 'Virtual City', which consists of a moderately sized network, generated so as to resemble land use patterns, travel behavior, and activity patterns observed in Singapore (Basu et al., 2018, 2021), with calibrated parameters such as time-of-day, mode,

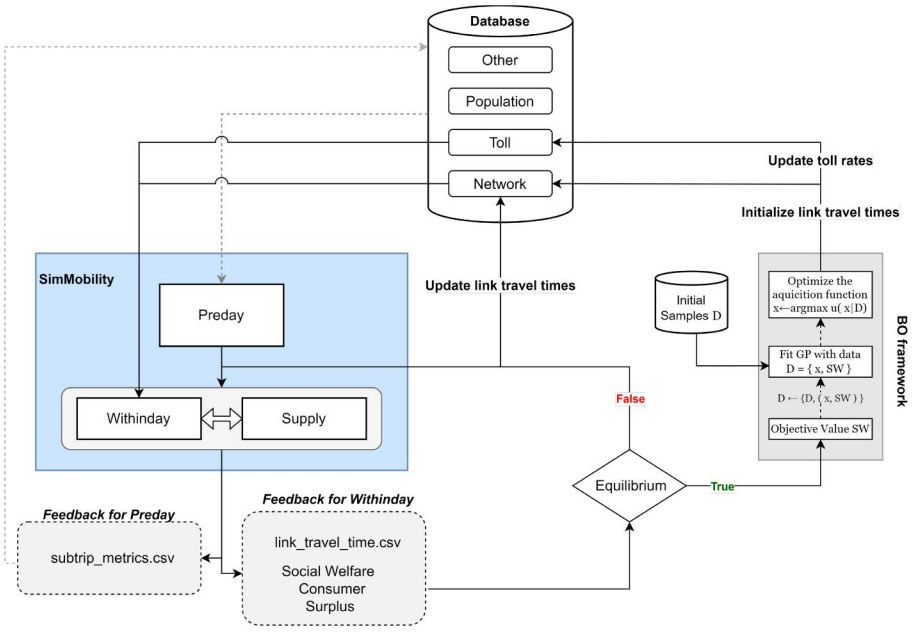

Figure 5. SimMobility and Bayesian optimization for road pricing.

Table 1. Simulation parameters for tradable mobility credits analysis.

Variable description	Value
Departure time window	60-minute time interval around the preferred departure time
Departure time interval	5 min
Day-to-day learning rate	0.2
Token allocation rate	1 credit every 20 min
Token lifetime	1420 min
Initial credit price	0.1 $
Initial credit allocation	72 credits
Maximum credit cost per trip	160 credits
Transaction fees	0 $

destination choice, route choice, speed-density parameters, zone-to-zone travel time, etc. The road network consists of 95 nodes (intersections), 286 segments (road sections with homogeneous geometry), and 254 links (groups of one or more segments with similar properties). The population subset used contains 19,000 private car drivers. Among the daily activity schedule given by *Preday*, 85% of the trips are work-related, 10% are education related and the rest are for other purposes (like shopping); on average, every person has 1.04 tours and 2.6 trips per day.

In this study, we perform 25 iterations (i.e., days) of the within-day learning for each toll evaluation to ensure that the demand and supply are consistent to a certain degree. We investigate the within-day behavior for an average weekday, including departure time and route choices and all TCS-related transactions. The pre-day daily activity schedule (by half-hour slots) is predetermined and fixed during the simulation (Basu et al., 2021).

We generate the value of time using the log-normal distribution in Chen et al. (2023), which is extracted from the Integrated Public Use Microdata Series (IPUMS) 2019 census data (Ruggles et al., 2021). The average value of time is $13/hour. The ratios of schedule delay early and late penalties to the value of time are assumed to follow triangular distributions with modes at 0.5 and 2, respectively, bounded by the widely used trip timing preferences relationship, i.e., the schedule delay early parameter is half of the value of time, which is in turn half that of the schedule delay late parameter (Small, 2012, Vickrey, 1969). Further, Table 1 presents simulation parameters used for the TCS experiments. The presented values are only one feasible combination to showcase the functionality of the simulation framework, and their influence should be further explored in other TCS design assessments in future work.

5.2. Base scenario

We first examine the properties of the day-to-day process for our 'Virtual City', under no TCS. Initially,

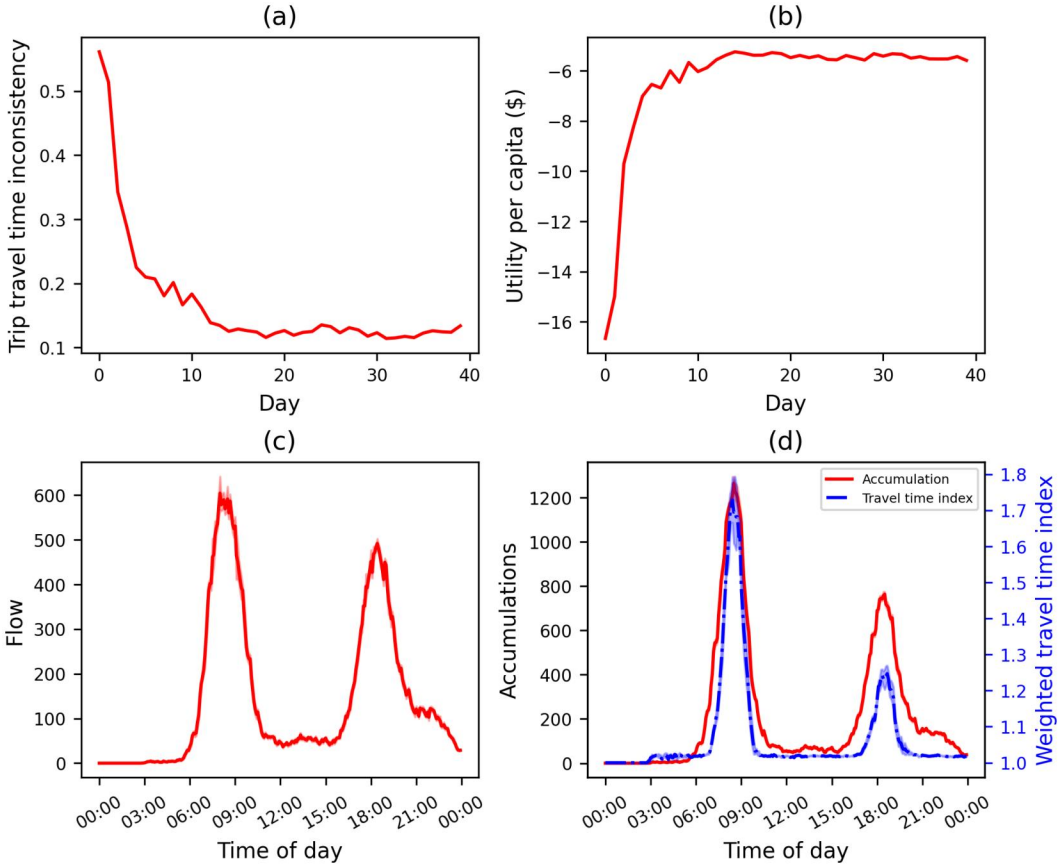

Figure 6. The evolution process with no toll: (a) trip travel time inconsistency; (b) utility per capita; (c) departure flow by 5-min intervals; (d) average accumulation (red) and weighted travel time index (blue).

travelers use the free-flow link travel times as their travel time estimates. After each simulated day, these estimates are updated based on the actual travel times experienced, with more recent days given higher weight. These updated values are then used as the predicted travel times for the next day's route choice.

To assess convergence of this day-to-day learning process, we measure the inconsistency between the predicted trip travel time (calculated as the sum of the predicted travel times for each link on the chosen route) and the actual trip travel time experienced during simulation. A decreasing inconsistency over time indicates that the system is converging.

The inconsistency is calculated as $\sum_n \sum_i^{I_n} |T^{\text{sim}}_{n,i,d} - T^{\text{pre}}_{n,i,d}| / \sum_n \sum_i^{I_n} T^{\text{sim}}_{n,i,d}$, where $T^{\text{sim}}_{n,i,d}$ is the simulated travel time of traveler n's ith trip on day d, and $T^{\text{pre}}_{n,i,d}$ is the predicted travel time.

Figure 6(a) presents the convergence of the trip travel time. It is found that the inconsistency becomes stable around 0.15 after day 15, implying that the day-to-day evolution process achieves stationarity and an acceptable degree of consistency. Figure 6(b) shows the evolution process of the experienced utility per capita. Again, convergence is observed with small variability across iterations. We perform a commonly used stationary test, the Augmented Dickey-Fuller (ADF) test (Cheung & Lai, 1995), on the utility data to examine the stationarity. If the p-value of the test is smaller than 0.05, the null hypothesis is rejected, i.e., the tested data does not have a unit root and it is called a stationary series. In this experiment, we have a p-value $\ll$ 0.05 hence stationarity is achieved. Figure 6(c) illustrates the (car-based) departure rates for all activity purposes by 5-min intervals of an average day, clearly displaying the morning and evening peak periods, wherein the curve shows the average values across the last 10 days, and the shadow stands for the 95% confidence interval We also plot the accumulation and weighted travel time index to quantify the extent of congestion on the network. Accumulation is simply the number of vehicles on the network at a certain time interval. The travel time index (TTI) is the ratio of realized trip travel time to free-flow travel time.

The TTI is weighted by trip distance for every 5-min interval and computed as:

$$TTI_{\tilde{t}} = \frac{\sum_i \frac{Dist_i \cdot TT_i}{TT_i^{ff}}}{\sum_i Dist_i}, \forall i \text{ that } \tilde{t} - 1 < t_i < \tilde{t},$$

where t_i: departure time of trip i, $\tilde{t}$: time interval, $Dist_i$: distance of trip i, TT_i: experienced travel time of trip i, TT_i^{ff}: free-flow travel time of trip i.

In Figure 6(d), the red curve represents the average accumulation across the last 10 days at 5-min resolution and the shadow area the 95% confidence interval are presented. Similarly, the blue curve represents the weighted TTI, with peaks of 1.8 in the morning and 1.3 in the evening. In Argyros et al. (2023), where an identical basecase used, a toll that improves social welfare was only found to exist during the morning peak. Thus, here our focus is on utilizing BO to design a distance-based toll that targets the morning peak.

5.3. TCS scenario

In this section, we present the simulation results under a distance-based credit step tariff. To design the tariff, we used Bayesian optimization which ran for 30 toll iterations. We then chose the one that yielded the highest social welfare. As presented in Section 4.2 a Gaussian curve is used to generate the toll. Here the optimal toll has a peak (μ_g) at 8:59 in the morning, with an amplitude of 0.0194 credits per kilometer and 72 min standard deviation. Utilizing this profile, we generate the tariff for each five-minute interval. The evolution process is shown in Figure 7.

The inconsistency of trip travel time reduces and becomes stable around 0.1 after day 15, as presented in Figure 7(a). We plot the social welfare gains per capita in Figure 7(b), which is computed as the average difference of the simulated individual specific utilities between the TCS case and base case. The average social welfare gains per capita (driver) of the last 10 days is \$0.38, with a 95% confidence interval of [\$0.3, \$0.46]. Figure 7(d) shows the flows (red curve for base scenario and blue curve for TCS scenario) and tariff profile (colored in grey). We plot the flows of the morning peak for better illustration in Figure 8. Clearly, the flow curve is flattened as the demand shifts to earlier intervals to avoid the larger credit charges. Consequently, as shown in Figure 7(f), the peak accumulation reduces from around 1200 vehicles to 800 vehicles, and congestion is mitigated as reflected by the reduction of the weighted TTI from 1.8 to 1.35, leading to gains in social welfare. Figure 7(c) displays the evolution of the credit price, which stabilizes at \$0.041. The result is consistent with the evolution of the credit transactions on an average day plotted in Figure 7(e), where the numbers of sold and bought credits reach the same level. The jump in the curve of accumulative buying transactions stand for the morning peak of departures in the flow.

In addition to Figure 8, we further plot the individual shifts in departure time in Figure 9 from the base scenario to the TCS scenario. Times on both sides of the figure represent the trip start time of a 30-minute interval (e.g., 06:30:00 represents the time interval [6:30,7:00]). The widths of an arc or time-interval are proportional to their quantity with respect to the total demand. Before the peak of the credit tariff, i.e., before 9:00, it is observed that arcs connecting to an early time interval are thicker compared to those connecting to a later interval, indicating that most behavior shifts are earlier departure choices, avoiding higher credit charges. Similarly, after the tariff peak (after 9:30), more travelers postpone their trips.

We also evaluate the changes in schedule delay costs for both the base and TCS scenarios in Figure 10(a) for the full day and Figure 10(b) for the morning peak. The x-axis represents the 30-minute interval of the preferred arrival time, and the y-axis is the schedule delay cost per trip in the corresponding time interval. Note that the average trip travel time is 7.7 min and 95% of trip travel time is smaller than 17 min, hence most trips start and end within the same 30-minute interval. Before the tariff peak (8:00), the sums of the schedule delay early and schedule delay late costs in TCS scenario are close to those in the base case, while the proportion of schedule delay early clearly increases, due to earlier departure times. During the peak, schedule delay late cost is significantly reduced thanks to the savings in travel time. After the peak (9:30), though we observe a few trip postponements in both Figures 8 and 9, the schedule delay late costs do not increase significantly as travel time is reduced.

Another critical characteristic of a TCS system that needs to be investigated is trading behavior in the market. As shown in Figure 11(a), buying transactions only happen in the peak hour since travelers can only buy credits at the time of departure if they are short of credits. In contrast, the selling transactions happen across the day. For travelers who sell at the beginning of the day, most of them sell at full wallets as shown in Figure 11(b), where the average trading amount is close to the full wallet (72 credits). In addition, relatively large amount of selling is observed during the peak hours. This is because of the selling model which requires a predicted toll that may be inaccurate

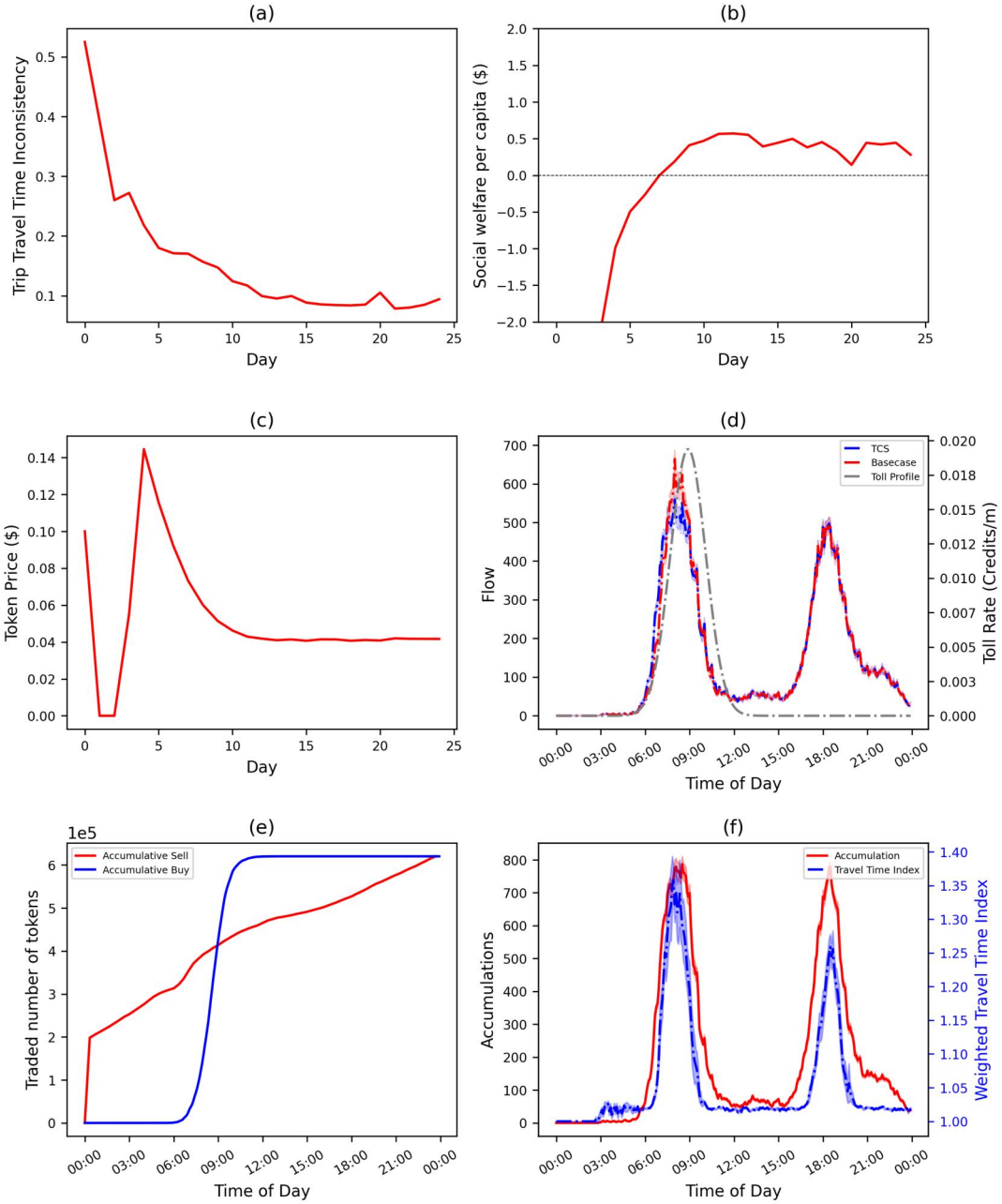

Figure 7. The evolution process with a distance-based credit toll: (a) trip travel time inconsistency; (b) social welfare per capita; (c) token price; (d) departure flow by 5-min intervals; (e) accumulated traded number of tokens; (f) average accumulation (red) and weighted travel time index (blue).

because the chosen path and departure time is not known before the choice is made. For most of the trips, the realized credit charge is smaller than the predicted one, thus the selling profit becomes positive after the departure time is chosen, triggering a selling decision according to the selling model in Section 2.3. The other instances of selling are scattered across the day with an increase toward the end of the day. Fluctuations occur due the tariff profile, which has multiple (5-min) steps and that the tariff step is not a multiple of the credit allocation per time interval. In the work of Chen et al. (2023), travelers have just a single trip, a high resolution (every minute) of credit allocation, and a toll with five steps. There, the selling pattern observed here (high number of transactions at the beginning of the day, the early morning, and during peak hours) is also present, but with fewer fluctuations since the factors mentioned above are absent.

Moreover, it is found in Figure 11(b) that there are many selling transactions with small amounts of

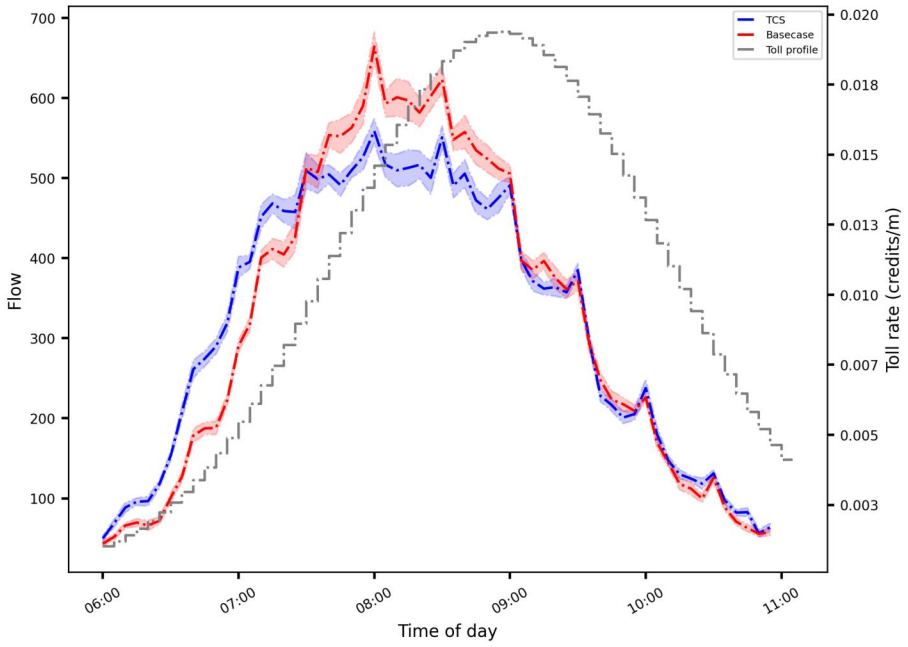

Figure 8. The flows of the morning peak.

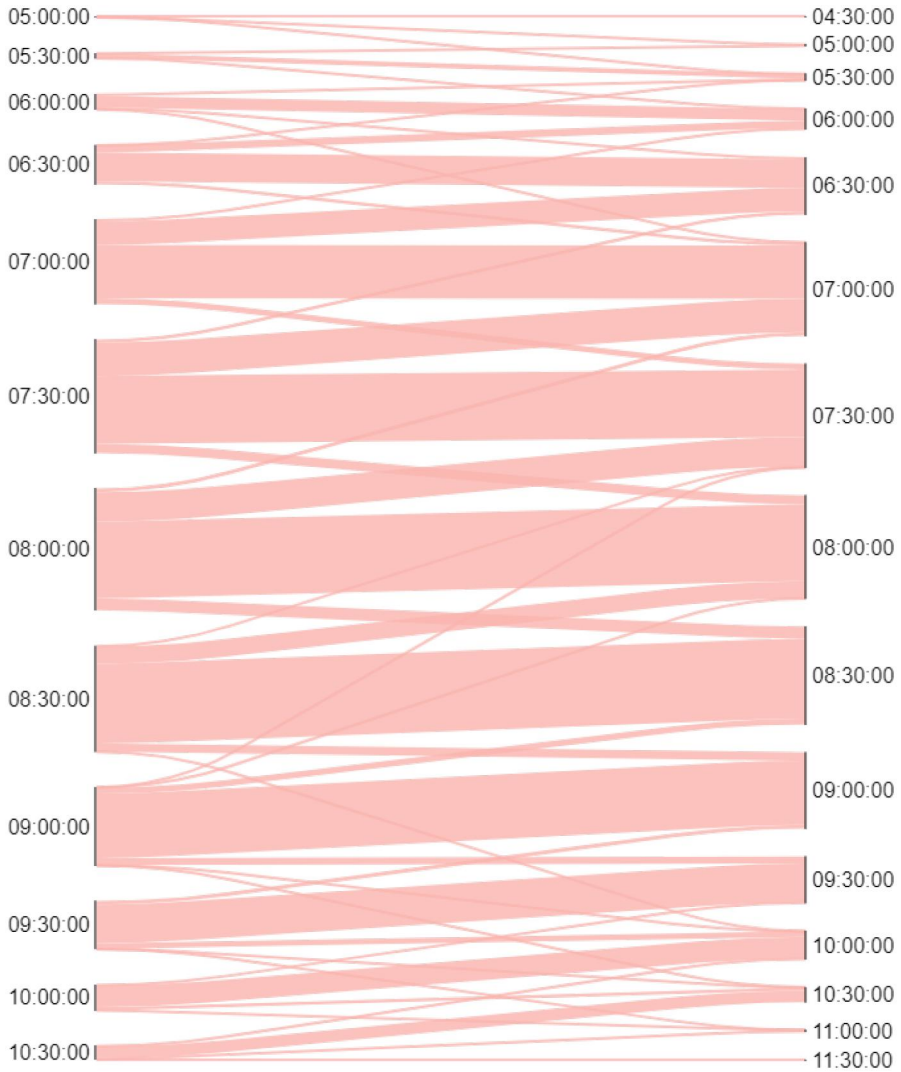

Figure 9. Changes in departure time, from base (left) to TCS (right) scenarios.

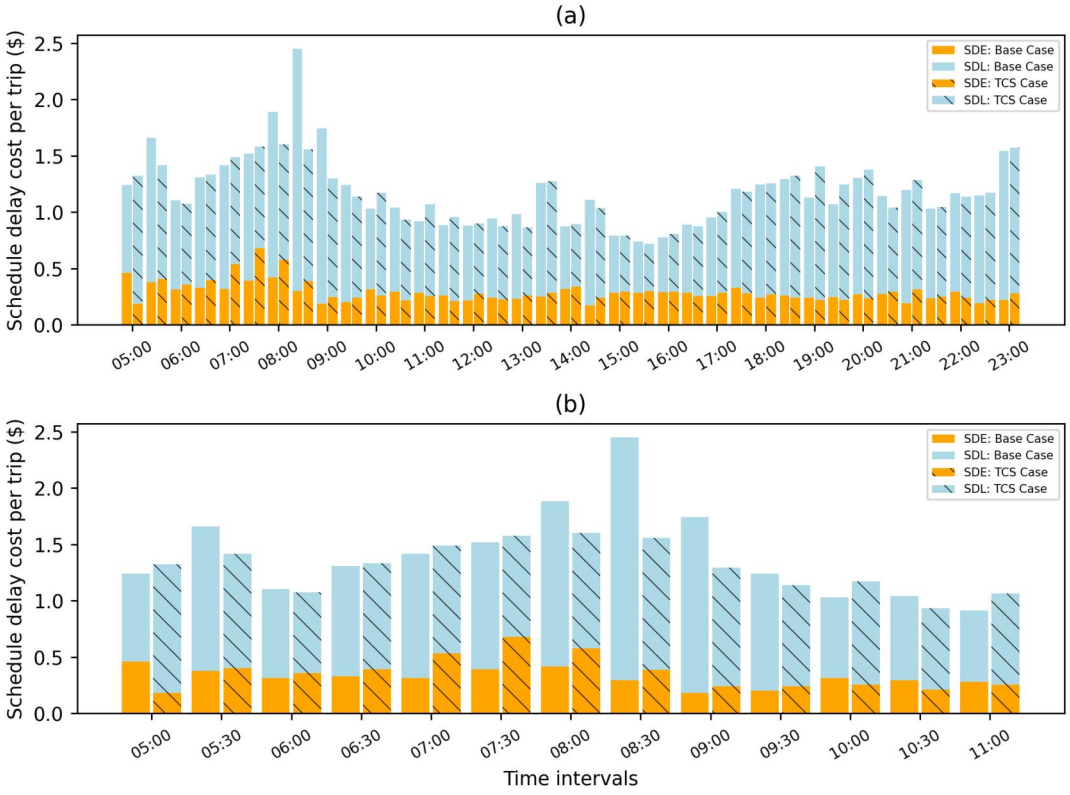

Figure 10. Schedule delay cost in base and TCS scenarios: (a) full day; (b) morning period only.

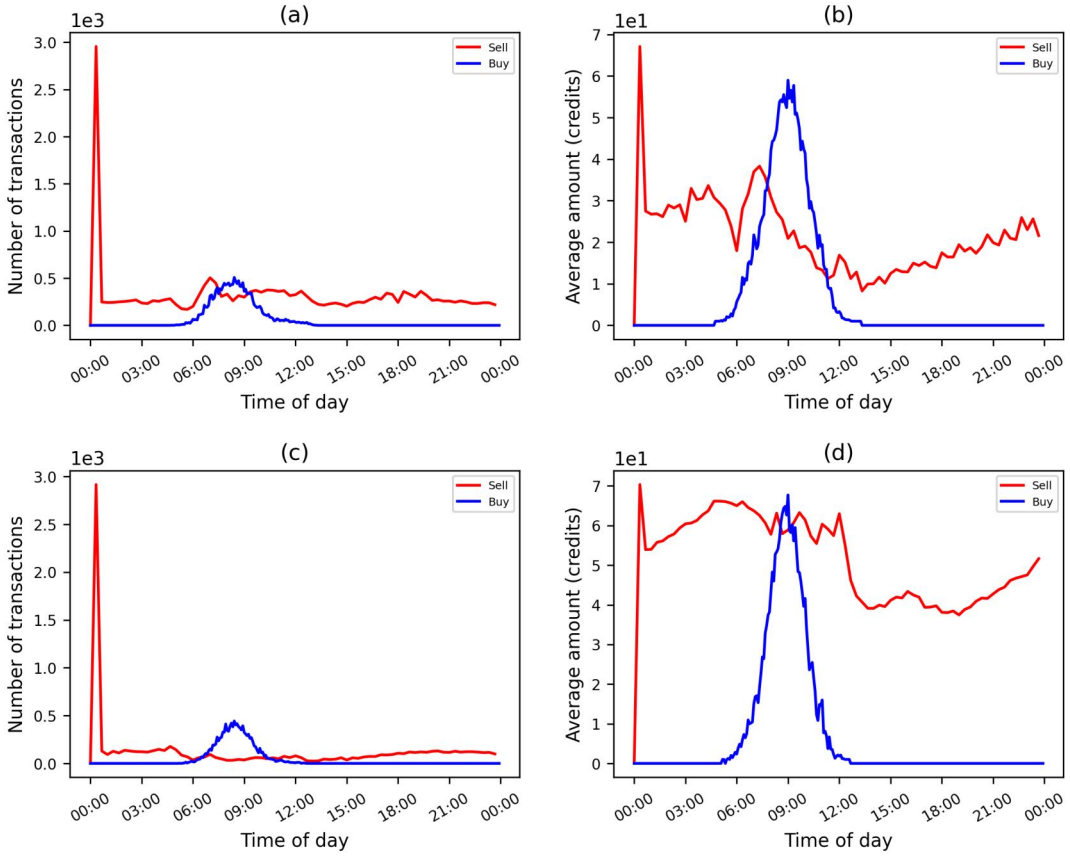

Figure 11. The transaction numbers (left) and average trading amount (right) with (bottom) and without (top) a profit threshold.

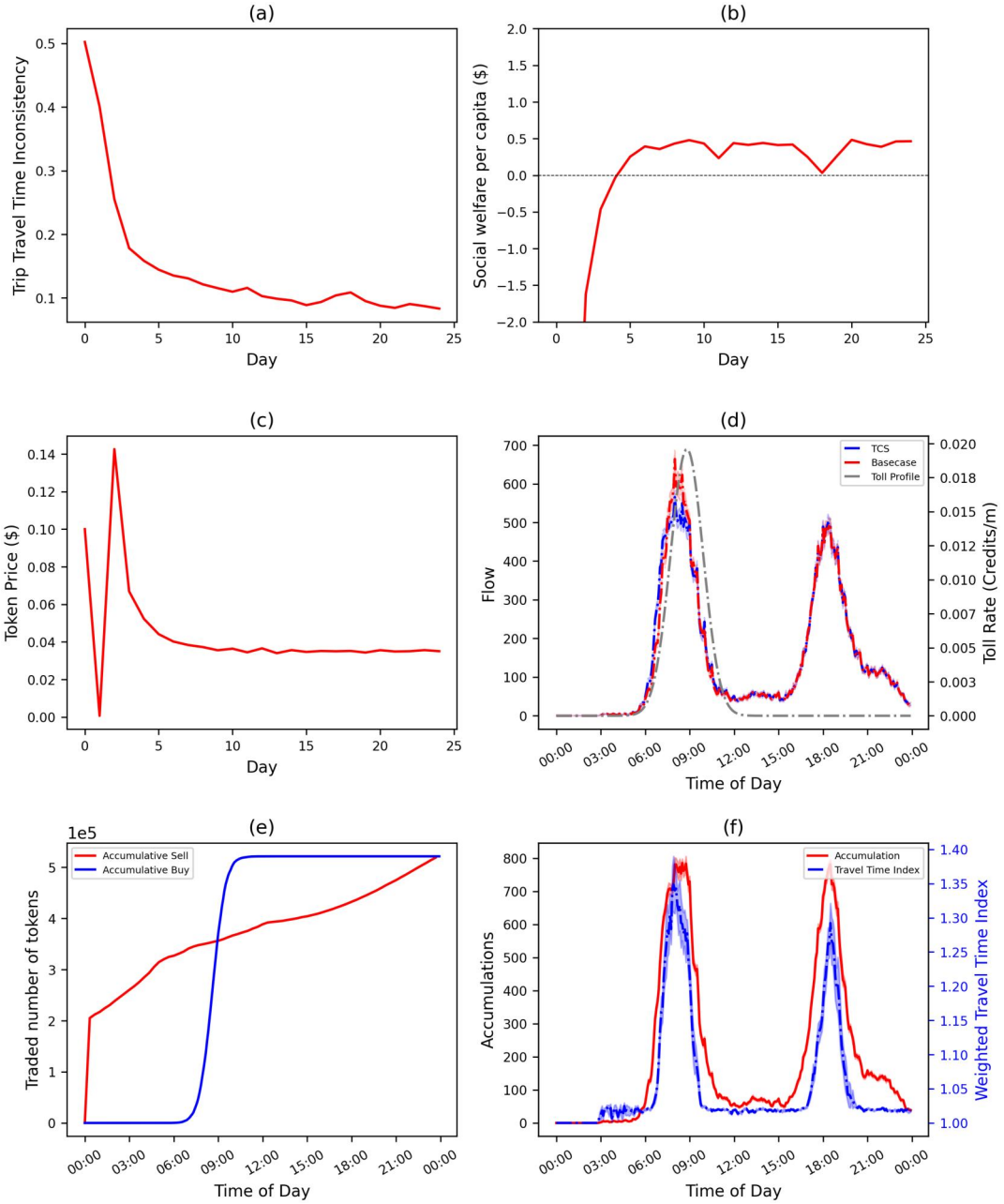

Figure 12. The evolution process of TCS with a profit threshold.

Figure 13. Average network density improvement from the basecase (left) to the TCS case with profit threshold (right) during the peak hour (8:00–9:00) for an average day at stability.

Table 2. Statistics of the TCS with and without profit threshold.

Factors	Without	With
Profit threshold	0	$1
Sell No. Trans.	22780	8992
Buy No. Trans.	16852	12173
Traded credits	1.24×10^6	1.04×10^6
Travelers with buyback	4881	1651
Welfare gain	$0.38($\pm$0.08)	$0.36($\pm$0.1)
Credit price	$0.041	$0.035
Tariff profile	(8:59, 72, 0.0194)	(8:54, 66, 0.0196)

credits (smaller than 20 credits), as well as the phenomenon of selling followed by subsequent buying (termed buyback). This is undesirable because if the credit system is used by certain individuals to make a profit *via* speculation, it could hamper the acceptability of such a system. To prevent such undesirable market behaviors, Brands et al. (2020) propose to use a small transaction fee to suppress the frequent selling. Alternatively, we propose to set up a threshold on the selling profit. In particular, travelers are only allowed to sell credits if the current selling profit is larger than the predetermined threshold. A threshold of $1 is adopted in this study and the BO is used again to design the optimal toll profile. A similar toll was detected (μ_g : 8:54, A_g : 0.0196 and σ_g : 66) and the evolution process under the new tariff is shown in Figure 12. Besides the convergence, we observe similar social welfare gains, departure flow, accumulation and weighted TTI. The stable credit price is $0.035, which is lower than that of the case without the profit threshold, caused by the changes in toll shape and selling behaviors and the resulted departure time choices.

In Figure 12(e), it is worth noting that the total number of traded credits is significantly reduced compared to that in Figure 7(e).

Leveraging the detailed network of our simulator, we illustrate the improvement achieved from the introduction of a TCS scheme in the network's density level in Figure 13, with the toll clearly alleviating network congestion bottlenecks. Lastly, we summarize the relevant factors such as numbers of transactions, traded credits, and travelers with buyback behavior, social welfare gain, and credit price in Table 2. As desired and expected, after imposing a small profit threshold, the number of transactions is greatly reduced, and fewer travelers have the buyback behavior. Also, the average trading amount of credits is found to be larger, as shown in Figure 11(d) and (b). Social welfare is similar, but slightly decreased, compared to the no profit threshold case. One may expect that the resulting lower credit price could cause a fewer shift of departures in periods with relatively lower tariffs, however here the effect of the threshold in the social welfare gains seems to be minimal. Nevertheless, imposing a profit threshold is an effective way to control undesirable trading behaviors. More comprehensive experiments are needed to test the price elasticity and compare the performance of transaction fees and the profit threshold. Lastly, for verification purposes, we conducted three replications of the threshold case using different random seeds in the simulator. The resulting standard deviation was small, indicating that the outcomes were consistent across the runs, with similar values observed in each replication.

6. Conclusions

This paper proposes a flexible simulation framework, implemented in a modular and extensible way in a state-of-the-art agent- and activity-based simulator, for the detailed modeling and assessment of TCS. Demand is modeled using an activity-based model and a within-day departure and route choice model sensitive to individual credit charges and heterogeneous preferences. Transportation supply is represented by a multi-modal mesoscopic network model and is extended with TCS capabilities for handling all credit transactions within the simulation. This proposed framework allows for the simulation of a variety of TCS design schemes and a selected recent TCS design was here tested and its properties validated for showcasing in a prototypical urban setting.

The results show convergence of the day-to-day process in terms of trip travel time, credit price, flow pattern, and travel utility and validate the general properties of TCS previously demonstrated in theoretical models. As expected, and thanks to the suitability of BO for complex simulation-based optimization, an optimized credit tariff triggers the demand shift in peak hours to alleviate overall congestion and improves social welfare compared to the no-toll case. Moreover, the results suggest that a small profit threshold is able to effectively control undesirable trading behaviors such as frequent selling and buyback.

It should be pointed out that the current TCS results, including the welfare gain estimates do not yet account for behavior changes in the pre-day activity-based model and therefore ignore possible shifts in activity types, number, duration, time of day, destination, and mode choice; this constitutes an important avenue for future assessment using our framework. In addition, the proposed simulation framework makes it

possible to model complex market designs, individual market behaviors, and networks, thereby contributing substantially to the assessment of TCS properties and impacts of alternative demand management mechanisms (Liu et al., 2024) and heterogeneous market behaviors (Dogterom et al., 2017). Such alternative designs and possible behaviors including loss aversion, risk aversion and endowment effects should be examined in more detail. Finally, the performance of TCS under demand and supply variability and uncertainty is also an avenue for exploration with our proposed framework, especially in large-scale simulations as investigated for pricing strategies in Jing et al. (2024).

Notes

1. https://github.com/smart-fm/simmobility-prod.

Disclosure statement

No potential conflict of interest was reported by the author(s).

Funding

This research was partially carried out under (a) the NEMESYS project funded by the Technical University of Denmark (DTU) – Nanyang Technical University (NTU) Alliance, and (b) in its last stage, under the EU's Horizon Europe's FEDORA project, grant agreement No. 101203465.

References

Adnan, M., Pereira, F. C., Azevedo, C. M. L., Basak, K., Lovric, M., Raveau, S., & Ben-Akiva, M. (2016). *Simmobility: A multi-scale integrated agent-based simulation platform* [Paper presentation]. 95th Annual Meeting of the Transportation Research Board Forthcoming in Transportation Research Record. Transportation Research Board.

Alogdianakis, F., Gkartzonikas, C., & Dimitriou, L. (2024). Development of a credit scheme for managing mobility in university communities: Results from a feasibility study. *Research in Transportation Business & Management*, *53*, 101106. https://doi.org/10.1016/j.rtbm.2024.101106

Anda, C., Erath, A., & Fourie, P. J. (2017). Transport modelling in the age of big data. *International Journal of Urban Sciences*, *21*(sup1), 19–42. https://doi.org/10.1080/12265934.2017.1281150

Argyros, D., Liu, R., Seshadri, R., Rodrigues, F., & Azevedo, C. L. (2023). Bayesian optimization of road pricing using agent-based mobility simulation [Paper presentation]. 11th Symposium of the European Association for Research in Transportation, Zurich, Switzerland.

Azevedo, C. L., Deshmukh, N. M., Marimuthu, B., Oh, S., Marczuk, K., Soh, H., Basak, K., Toledo, T., Peh, L.-S., & Ben-Akiva, M. E. (2017). Simmobility short-term: An integrated microscopic mobility simulator. *Transportation Research Record: Journal of the Transportation Research Board*, *2622*(1), 13–23. https://doi.org/10.3141/2622-02

Balzer, L., & Leclercq, L. (2022). Modal equilibrium of a tradable credit scheme with a trip-based MFD and logit-based decision-making. *Transportation Research Part C: Emerging Technologies*, *139*, 103642. https://doi.org/10.1016/j.trc.2022.103642

Balzer, L., Ameli, M., Leclercq, L., & Lebacque, J.-P. (2023). Dynamic tradable credit scheme for multimodal urban networks. *Transportation Research Part C: Emerging Technologies*, *149*, 104061. https://doi.org/10.1016/j.trc.2023.104061

Bao, H. X., & Ng, J. (2022). Tradable parking permits as a transportation demand management strategy: A behavioural investigation. *Cities*, *120*, 103463. https://doi.org/10.1016/j.cities.2021.103463

Basu, R., Araldo, A., Akkinepally, A. P., Nahmias Biran, B. H., Basak, K., Seshadri, R., Deshmukh, N., Kumar, N., Azevedo, C. L., & Ben-Akiva, M. (2018). Automated mobility-on-demand vs. mass transit: A multi-modal activity-driven agent-based simulation approach. *Transportation Research Record: Journal of the Transportation Research Board*, *2672*(8), 608–618. https://doi.org/10.1177/0361198118758630

Basu, R., Ferreira, J., & Ponce-Lopez, R. (2021). A framework to generate virtual cities as sandboxes for land use-transport interaction models. *Journal of Transport and Land Use*, *14*(1), 303–323. https://doi.org/10.5198/jtlu.2021.1791

Ben-Akiva, M. E., & Bierlaire, M. (2003). Discrete choice models with applications to departure time and route choice. In *Handbook of transportation science*. Kluwer Academic Publishers. https://api.semanticscholar.org/CorpusID:119743124

Ben-Akiva, M., Bierlaire, M., Koutsopoulos, H. N., & Mishalani, R. (2002). Real time simulation of traffic demand-supply interactions within dynamit. In *Transportation and network analysis: current trends* (pp. 19–36). Springer. https://doi.org/10.1007/978-1-4757-6871-8_2

Bowman, J. L., & Ben-Akiva, M. E. (2001). Activity-based disaggregate travel demand model system with activity schedules. *Transportation Research Part A: Policy and Practice*, *35*(1), 1–28. https://doi.org/10.1016/S0965-8564(99)00043-9

Brands, D. K., Verhoef, E. T., Knockaert, J., & Koster, P. R. (2020). Tradable permits to manage urban mobility: Market design and experimental implementation. *Transportation Research Part A: Policy and Practice*, *137*, 34–46. https://doi.org/10.1016/j.tra.2020.04.008

Cantarella, G. E., & Cascetta, E. (1995). Dynamic processes and equilibrium in transportation networks: Towards a unifying theory. *Transportation Science*, *29*(4), 305–329. https://doi.org/10.1287/trsc.29.4.305

Chen, S., Seshadri, R., Azevedo, C. L., Akkinepally, A. P., Liu, R., Araldo, A., Jiang, Y., & Ben-Akiva, M. E. (2023). Market design for tradable mobility credits.

Transportation Research Part C: Emerging Technologies, *151*, 104121. https://doi.org/10.1016/j.trc.2023.104121

Cheung, Y.-W., & Lai, K. S. (1995). Lag order and critical values of the augmented Dickey–Fuller test. *Journal of Business & Economic Statistics*, *13*(3), 277–280. https://doi.org/10.2307/1392187

de Palma, A., & Lindsey, R. (2020). Tradable permit schemes for congestible facilities with uncertain supply and demand. *Economics of Transportation*, *21*, 100149. https://doi.org/10.1016/j.ecotra.2019.100149

de Palma, A., Proost, S., Seshadri, R., & Ben-Akiva, M. (2018). Congestion tolling-dollars versus tokens: A comparative analysis. *Transportation Research Part B: Methodological*, *108*, 261–280. https://doi.org/10.1016/j.trb.2017.12.005

Dogterom, N., Ettema, D., & Dijst, M. (2017). Tradable credits for managing car travel: A review of empirical research and relevant behavioural approaches. *Transport Reviews*, *37*(3), 322–343. https://doi.org/10.1080/01441647.2016.1245219

Fan, W., & Jiang, X. (2013). Tradable mobility permits in roadway capacity allocation: Review and appraisal. *Transport Policy*, *30*, 132–142. https://doi.org/10.1016/j.tranpol.2013.09.002

Fan, W., Xiao, F., & Nie, Y. (2022). Managing bottleneck congestion with tradable credits under asymmetric transaction cost. *Transportation Research Part E: Logistics and Transportation Review*, *158*, 102600. https://doi.org/10.1016/j.tre.2021.102600

Goddard, H. C. (1997). Using tradeable permits to achieve sustainability in the world's large cities: Policy design issues and efficiency conditions for controlling vehicle emissions, congestion and urban decentralization with an application to Mexico city. *Environmental and Resource Economics*, *10*(1), 63–99. https://doi.org/10.1023/A:1026444113237

Grant-Muller, S., & Xu, M. (2014). The role of tradable credit schemes in road traffic congestion management. *Transport Reviews*, *34*(2), 128–149. https://doi.org/10.1080/01441647.2014.880754

Guo, R.-Y., Huang, H.-J., & Yang, H. (2019). Tradable credit scheme for control of evolutionary traffic flows to system optimum: Model and its convergence. *Networks and Spatial Economics*, *19*(3), 833–868. https://doi.org/10.1007/s11067-018-9432-z

Hamm, L. S., Weikl, S., Loder, A., Bogenberger, K., Schatzmann, T., & Axhausen, K. W. (2023). *Mobilitycoins: First empirical findings on the user-oriented system design for tradable credit schemes* [Paper presentation]. 102nd Annual Meeting of the Transportation Research Board (Trb 2023), Washington, DC.

Jing, P., Seshadri, R., Sakai, T., Shamshiripour, A., Alho, A. R., Lentzakis, A., & Ben-Akiva, M. E. (2024). Evaluating congestion pricing schemes using agent-based passenger and freight microsimulation. *Transportation Research Part A: Policy and Practice*, *186*, 104118. https://doi.org/10.1016/j.tra.2024.104118

Kamargianni, M., Yfantis, L., Muscat, J., Azevedo, C., & Ben-Akiva, M. (2019). *Incorporating the mobility as a service concept into transport modelling and simulation frameworks* [Paper presentation]. Special Report-National Research Council, Transportation Research Board, Washington, DC.

Lessan, J., & Fu, L. (2022). Credit-and permit-based travel demand management state-of-the-art methodological advances. *Transportmetrica A: Transport Science*, *18*(1), 5–28. https://doi.org/10.1080/23249935.2019.1692963

Lindsey, R. (2006). Do economists reach a conclusion? *Econ Journal Watch*, *3*(2), 292–379.

Liu, R., Chen, S., Jiang, Y., Seshadri, R., Ben-Akiva, M., & Lima Azevedo, C. (2023). Managing network congestion with a trip-and area-based tradable credit scheme. *Transportmetrica B: Transport Dynamics*, *11*(1), 434–462. https://doi.org/10.1080/21680566.2022.2083034

Liu, R., Jiang, Y., & Azevedo, C. L. (2020). *Bayesian optimization of area-based road pricing* [Paper presentation]. 7th International IEEE Conference on Models and Technologies for Intelligent Transportation Systems. IEEE.

Liu, R., Wang, D. Z., Jiang, Y., Seshadri, R., & Azevedo, C. L. (2024). Tradable credit schemes with peer-to-peer trading mechanisms. *Transportation Research Part C: Emerging Technologies*, *160*, 104532. https://doi.org/10.1016/j.trc.2024.104532

Liu, W., Yang, H., Yin, Y., & Zhang, F. (2014). A novel permit scheme for managing parking competition and bottleneck congestion. *Transportation Research Part C: Emerging Technologies*, *44*, 265–281. https://doi.org/10.1016/j.trc.2014.04.005

Lombardi, C., Annaswamy, A. M., & Picado-Santos, L. (2023). Model-based dynamic toll pricing scheme for a congested suburban freeway with multiple access locations. *Journal of Intelligent Transportation Systems*, *27*(6), 693–720. https://doi.org/10.1080/15472450.2022.2075702

Lu, Y., Adnan, M., Basak, K., Pereira, F. C., Carrion, C., Saber, V. H., & Ben-Akiva, M. E. (2015a). *Simmobility mid-term simulator: A state of the art integrated agent based demand and supply model* [Paper presentation]. 94th Annual Meeting of the Transportation Research Board, Washington, DC.

Lu, Y., Seshadri, R., Pereira, F., O'Sullivan, A., Antoniou, C., & Ben-Akiva, M. (2015b). Dynamit2. 0: Architecture design and preliminary results on real-time data fusion for traffic prediction and crisis management. In *2015 IEEE 18th International Conference on Intelligent Transportation Systems* (pp. 2250–2255). IEEE.

Miralinaghi, M., & Peeta, S. (2016). Multi-period equilibrium modeling planning framework for tradable credit schemes. *Transportation Research Part E: Logistics and Transportation Review*, *93*, 177–198. https://doi.org/10.1016/j.tre.2016.05.013

Miralinaghi, M., & Peeta, S. (2018). A multi-period tradable credit scheme incorporating interest rate and traveler value-of-time heterogeneity to manage traffic system emissions. *Frontiers in Built Environment*, *4*, 33. https://doi.org/10.3389/fbuil.2018.00033

Nie, Y. M. (2012). Transaction costs and tradable mobility credits. *Transportation Research Part B: Methodological*, *46*(1), 189–203. https://doi.org/10.1016/j.trb.2011.10.002

Nielsen, O. A. (2004). Behavioral responses to road pricing schemes: Description of the Danish Akta experiment. *Journal of Intelligent Transportation Systems*, *8*(4), 233–251. https://doi.org/10.1080/15472450490495579

Provoost, J., Cats, O., & Hoogendoorn, S. (2023). Design and classification of tradable mobility credit schemes. *Transport Policy*, *136*, 59–69. https://doi.org/10.1016/j.tranpol.2023.03.010

Ruggles, S., Flood, S., Foster, S., Goeken, R., Pacas, J., Schouweiler, M., & Sobek, M. (2021). *Ipums usa: Version 11.0*. (Tech. Rep.). IPUMS.

Servatius, P., Loder, A., Provoost, J., Balzer, L., Cats, O., Leclercq, L., Hoogendoorn, S., & Bogenberger, K. (2023). Trading activity and market liquidity in tradable mobility credit schemes. *Transportation Research Interdisciplinary Perspectives*, *22*, 100970. https://doi.org/10.1016/j.trip.2023.100970

Seshadri, R., de Palma, A., & Ben-Akiva, M. (2022). Congestion tolling—dollars versus tokens: Within-day dynamics. *Transportation Research Part C: Emerging Technologies*, *143*, 103836. https://doi.org/10.1016/j.trc.2022.103836

Siyu, L. (2015). *Activity-based travel demand model: Application and innovation* [PhD thesis]. National University of Singapore.

Small, K. A. (2012). Valuation of travel time. *Economics of Transportation*, *1*(1–2), 2–14. https://doi.org/10.1016/j.ecotra.2012.09.002

Srinivas, N., Krause, A., Kakade, S. M., & Seeger, M. W. (2012). Information-theoretic regret bounds for Gaussian process optimization in the bandit setting. *IEEE Transactions on Information Theory*, *58*(5), 3250–3265. https://doi.org/10.1109/TIT.2011.2182033

Tian, Y., Chiu, Y.-C., & Sun, J. (2019). Understanding behavioral effects of tradable mobility credit scheme: An experimental economics approach. *Transport Policy*, *81*, 1–11. https://doi.org/10.1016/j.tranpol.2019.05.019

Verhoef, E., Nijkamp, P., & Rietveld, P. (1997). Tradeable permits: Their potential in the regulation of road transport externalities. *Environment and Planning B: Planning and Design*, *24*(4), 527–548. https://doi.org/10.1068/b240527

Vickrey, W. S. (1969). Congestion theory and transport investment. *American Economic Review*, *59*(2), 251–260.

Wörner, A., Tiefenbeck, V., Wortmann, F., Meeuw, A., Ableitner, L., Fleisch, E., & Azevedo, I. (2022). Bidding on a peer-to-peer energy market: An exploratory field study. *Information Systems Research*, *33*(3), 794–808. https://doi.org/10.1287/isre.2021.1098

Xiao, F., Long, J., Li, L., Kou, G., & Nie, Y. (2019). Promoting social equity with cyclic tradable credits. *Transportation Research Part B: Methodological*, *121*, 56–73. https://doi.org/10.1016/j.trb.2019.01.002

Xiao, L.-L., Liu, T.-L., & Huang, H.-J. (2021). Tradable permit schemes for managing morning commute with carpool under parking space constraint. *Transportation*, *48*(4), 1563–1586. https://doi.org/10.1007/s11116-019-09982-w

Yang, H., & Wang, X. (2011). Managing network mobility with tradable credits. *Transportation Research Part B: Methodological*, *45*(3), 580–594. https://doi.org/10.1016/j.trb.2010.10.002

Ye, H., & Yang, H. (2013). Continuous price and flow dynamics of tradable mobility credits. *Transportation Research Part B: Methodological*, *57*, 436–450. https://doi.org/10.1016/j.trb.2013.05.007

Zhang, F., Lu, J., & Hu, X. (2021). Tradable credit scheme design with transaction cost and equity constraint. *Transportation Research Part E: Logistics and Transportation Review*, *145*, 102133. https://doi.org/10.1016/j.tre.2020.102133

Zhu, Y., Diao, M., Ferreira, J., & Zegras, P. C. (2018). An integrated microsimulation approach to land-use and mobility modeling. *Journal of Transport and Land Use*, *11*(1), 633–659. https://doi.org/10.5198/jtlu.2018.1186

Appendix A

A traveler checks for two conditions when he or she is making a selling decision: (i) the selling profit $P_n^d(t)$ must be positive, and (ii) the profit from selling now must be higher than that obtained from selling at any other time until the next departure (i.e., $t' < t_{n,1,d}^{dep}$), which can be determined by examining the sign of the derivative of $P_n^d(t)$ with regard to t. Thus, we can compute both the profit value and its derivative to obtain the optimal selling strategy. We analyze the derivative of profit function (8) in cases with different outcomes of the indicator functions. For ease of demonstration, here we simplify $1(g(t_{n,i,d}^{dep}) > x_n^d(t_{n,i,d}^{dep}))$ as $1(t_{n,i,d}^{dep})$, and take the case of two trips, 1 and 2, as an example:

A. If $g(t_{n,1,d}^{dep}) \le x_n^d(t_{n,1,d}^{dep})$ and $g(t_{n,2,d}^{dep}) \le x_n^d(t_{n,2,d}^{dep})$, i.e., $1(t_{n,1,d}^{dep}) = 1(t_{n,2,d}^{dep}) = 0$, we have

$$P_n^d(t) = x_n^d(t) \cdot p_d \cdot (1 - \hat{f}_s) - f_s, \tag{1}$$

and the derivative,

$$\frac{\partial P_n^d(t)}{\partial t} = \begin{cases} 0, & \text{if } x_n^d(t) = l \cdot r, \\ r \cdot p_d \cdot (1 - \hat{f}_s) > 0, & \text{otherwise.} \end{cases} \tag{2}$$

This implies that the profit will increase until the account balance reaches the maximum amount of $l \cdot r$ (i.e., full wallet). Though the derivative is 0 at the full wallet state, there is no incentive for a traveler to defer the selling since the oldest credits start to expire. Hence, the selling (of all credits) happens at the full wallet state. It is noteworthy that when the fixed transaction fee $f_s = 0$, the selling profit at full wallet state is the same as the profit of any selling strategy that avoids credit expiration (e.g., selling every time new credits are allocated). A positive transaction fee can prevent frequent selling with a small number of credits (Brands et al., 2020; Chen et al., 2023).

B. If $g(t_{n,1,d}^{dep}) > x_n^d(t_{n,1,d}^{dep})$ and $g(t_{n,2,d}^{dep}) > x_n^d(t_{n,2,d}^{dep})$, i.e., $1(t_{n,1,d}^{dep}) = 1(t_{n,2,d}^{dep}) = 1$, we have

$$\begin{aligned} P_n^d(t) = {} & x_n^d(t) \cdot p_d \cdot (1 - \hat{f}_s) - f_s \\ & - ((g(t_{n,1,d}^{dep}) - x_n^d(t_{n,1,d}^{dep})) \cdot p_d \cdot (1 + \hat{f}_b) + f_b) \\ & - ((g(t_{n,2,d}^{dep}) - x_n^d(t_{n,2,d}^{dep})) \cdot p_d \cdot (1 + \hat{f}_b) + f_b), \end{aligned} \tag{3}$$

and the derivative as

$$\frac{\partial P_n^d(t)}{\partial t} = \begin{cases} -2r \cdot p_d \cdot (1 + \hat{f}_b) < 0, & \text{if } x_n^d(t) = l \cdot r, \\ r \cdot p_d \cdot (1 - \hat{f}_s) - 2r \cdot p_d \cdot (1 + \hat{f}_b) < 0, & \text{otherwise,} \end{cases} \tag{4}$$

which is always negative. This implies that the profit will decrease and thus selling at the current time is the

optimal strategy if the profit is positive.

C. If $g(t^{dep}_{n,1,d}) > x^d_n(t^{dep}_{n,1,d})$ and $g(t^{dep}_{n,2,d}) \leq x^d_n(t^{dep}_{n,2,d})$, i.e., $1(t^{dep}_{n,1,d}) = 1$ and $1(t^{dep}_{n,2,d}) = 0$, we have

$$P^d_n(t) = x^d_n(t) \cdot p_d \cdot (1 - \hat{f}_s) - f_s - ((g(t^{dep}_{n,1,d}) - x^d_n(t^{dep}_{n,1,d})) \cdot p_d \cdot (1 + \hat{f}_b) + f_b) \tag{5}$$

and the derivative as

$$\frac{\partial P^d_n(t)}{\partial t} = \begin{cases} -r \cdot p_d \cdot (1 + \hat{f}_b) < 0, & \text{if } x^d_n(t) = l \cdot r, \\ r \cdot p_d \cdot (1 - \hat{f}_s) - r \cdot p_d \cdot (1 + \hat{f}_b) \leq 0, & \text{otherwise.} \end{cases} \tag{6}$$

D. If $g(t^{dep}_{n,1,d}) \leq x^d_n(t^{dep}_{n,1,d})$ and $g(t^{dep}_{n,2,d}) > x^d_n(t^{dep}_{n,2,d})$, i.e., $1(t^{dep}_{n,1,d}) = 0$ and $1(t^{dep}_{n,2,d}) = 1$, we have

$$P^d_n(t) = x^d_n(t) \cdot p_d \cdot (1 - \hat{f}_s) - f_s - ((g(t^{dep}_{n,2,d}) - x^d_n(t^{dep}_{n,2,d})) \cdot p_d \cdot (1 + \hat{f}_b) + f_b). \tag{7}$$

and the derivative as

$$\frac{\partial P^d_n(t)}{\partial t} = \begin{cases} -r \cdot p_d \cdot (1 + \hat{f}_b) < 0, & \text{if } x^d_n(t) = l \cdot r, \\ r \cdot p_d \cdot (1 - \hat{f}_s) - r \cdot p_d \cdot (1 + \hat{f}_b) \leq 0, & \text{otherwise.} \end{cases} \tag{8}$$

For both cases *C* and *D*, the derivative is negative when the proportional transaction fees $\hat{f}_s$ and $\hat{f}_b$ are positive, i.e., a traveler should thus sell all credits now. Without transaction fees, the derivative becomes 0 when the account balance is not full, and the selling profits now or later are the same. Positive fixed transaction fees make selling at full wallet beneficial for the sake of transaction cost minimization, and positive proportional transaction fees make immediate selling preferable as the derivative becomes negative.

We can easily extend the above analysis for cases with multiple trips. For all future *I* trips:

A. if all the tolls in credits are smaller than the corresponding expected account balances, the derivative of profit function is • 0, if the current account balance is full, • positive, otherwise.
B. if more than one toll in credits is larger than the corresponding expected account balance, the derivative of profit function is always negative.
C. if there is only one toll in credit larger than the corresponding expected account balance, the derivative of profit function is • 0, if the proportional transaction fees are 0, • negative, otherwise.